Heliyon 10 (2024) e23870

Contents lists available at ScienceDirect

Heliyon

journal homepage: www.cell.com/heliyon

Intra-tumor ROS amplification by melatonin interferes in the apoptosis-autophagy-inflammation-EMT collusion in the breast tumor microenvironment

Nirmal Das [a], Sudeshna Mukherjee [a,b], Ankur Das [a], Payal Gupta [a], Amit Bandyopadhyay [a], Sreya Chattopadhyay [a,c,*]

[a] Department of Physiology, University of Calcutta, 92, A.P.C. Road, Kolkata, West Bengal 700009, India
[b] Department of Physiology and Allied Sciences, Amity Institute of Health Allied Sciences, Amity University, Uttar Pradesh, India
[c] Centre for Research in Nanoscience and Nanotechnology (CRNN), University of Calcutta, JD-2, Salt Lake, Sector III, Kolkata-700098, India

ARTICLE INFO

Keywords:
Breast cancer
Melatonin
Inflammation
ROS
Autophagy
EMT

ABSTRACT

Epidemiological as well as experimental studies have established that the pineal hormone melatonin has inhibitory effects on different types of cancers. Several mechanisms have been proposed for the anticancer activities of melatonin, but the fundamental molecular pathways still require clarity. We developed a mouse model of breast cancer using Ehrlich's ascites carcinoma (injected in the 4th mammary fat pad of female Swiss albino mice) and investigated the possibility of targeting the autophagy-inflammation-EMT colloquy to restrict breast tumor progression using melatonin as intervention. Contrary to its conventional antioxidant role, melatonin was shown to augment intracellular ROS and initiate ROS-dependent apoptosis in our system, by modulating the p53/JNK & NF-κB/pJNK expressions/interactions. Melatonin-induced ROS promoted SIRT1 activity. Interplay between SIRT1 and NF-κB/p65 is known to play a pivotal role in regulating the crosstalk between autophagy and inflammation. Persistent inflammation in the tumor microenvironment and subsequent activation of the IL-6/STAT3/NF-κB feedback loop promoted EMT and suppression of autophagy through activation of PI3K/Akt/mTOR signaling pathway. Melatonin disrupted NF-κB/SIRT1 interactions blocking IL-6/STAT3/NF-κB pathway. This led to reversal of pro-inflammatory bias in the breast tumor microenvironment and augmented autophagic responses. The interactions between p62/Twist1, NF-κB/Beclin1 and NF-κB/Slug were altered by melatonin to strike a balance between autophagy, inflammation and EMT, leading to tumor regression. This study provides critical insights into how melatonin could be utilized in treating breast cancer via inhibition of the PI3K/Akt/mTOR signaling and differential modulation of SIRT1 and NF-κB proteins, leading to the establishment of apoptotic and autophagic fates in breast cancer cells.

1. Introduction

Breast cancer is the most common cancer in women worldwide and is associated with very high mortality rate. Drug resistance and increased incidences of recurrence are two prime causes of treatment failure. For a more efficient management of the disease, targeting

* Corresponding author. Department of Physiology, University of Calcutta, 92, A.P.C. Road, Kolkata, West Bengal 700009, India.
E-mail addresses: sreyasaha@gmail.com, scphys@caluniv.ac.in (S. Chattopadhyay).

https://doi.org/10.1016/j.heliyon.2023.e23870
Received 12 March 2023; Received in revised form 21 November 2023; Accepted 14 December 2023
Available online 20 December 2023

the complex nexus of redox stress, inflammation, apoptosis, autophagy and epithelial to mesenchymal transition (EMT) in the breast tumor microenvironment could possibly provide better prognosis.

Reactive oxygen species (ROS) are normal by-products of a wide range of cellular processes which appear to cut both ways in cancer cells. There are multiple reports pointing to intracellular ROS suppression-induced tumor apoptosis [1–3], and, studies have also demonstrated that typical antioxidants, including N-acetyl L-cysteine (NAC) and vitamin E, markedly increased lung cancer progression and melanoma metastasis [4]. High levels of ROS in cancer cells promotes the activation of c-Jun *N*-terminal kinase (JNK) and DNA damage response, which leads to the development of a feedback loop with the redox active transcription factor p53 and converts p53-induced growth arrest/senescence to apoptosis [5].

The ubiquitously expressed NAD + -dependent deacetylase silent information regulator 1 (SIRT1) is involved in the control of inflammatory responses, and nuclear factor kappa B (NF-κB) is an important target for SIRT1. There appears to be an antagonistic crosstalk between NF-κB and SIRT1 signaling pathways where SIRT1 inhibits NF-κB directly by deacetylating its p65 subunit [6,7]. Accumulating evidence also suggests that SIRT1 suppresses inflammatory responses through activation of autophagy by blocking the PI3K/Akt/mTOR pathways [8]. Autophagy is unique in the sense that it not only removes oxidized/damaged proteins but also bulky ROS-generating organelles (such as mitochondria and peroxisome) to restrict further ROS production [9].

Inflammation driven NF-κB activation with concomitant release of inflammatory cytokines (IL-1β, IL-6 and TNF-α) in the tumor microenvironment has been implicated in the promotion of breast tumorigenesis [10]. Apart from acting as a master regulator of inflammation, NF-κB/p65 also acts as an anti-apoptotic molecule through the inhibition of JNK activation by suppressing the build-up of ROS [11–13]. Also, NF-κB dependent IL-6 gene expression activates STAT3 and triggers its nuclear translocation, which in turn initiates transcriptional activation of genes (*bcl-2, mmp 2, mmp 9, vimentin*) associated with tumor cell survival and progression [14–16].

Mouse experiments have recognized certain links between compromised autophagy and tumorigenesis, with unchecked cell cycle progression and buildup and activation of oncoproteins [17,18]. The molecule central to regulating autophagy is the mammalian target of rapamycin (mTOR), downstream of PI3K/Akt, which often remains activated in certain types of cancers, and is linked with malignant transformation, apoptotic resistance and cell survival [19,20]. Hyper-activated PI3K/Akt pathway is also associated with the loss of PTEN (a phosphoinositide phosphatase that acts as a tumor suppressor) function [21,22]. Elevated migratory and invasive properties of breast cancer is closely related to NF-κB activation and expressions of the epithelial-to-mesenchymal transition transcription factors Snail, Slug, Twist and Zeb; acquisition of mesenchymal morphology; reduced expression of E-cadherin and increased expression of vimentin and/or fibronectin [23].

Melatonin (*N*-acetyl-5-methoxytryptamine) is an endogenous indole tryptophan derivative, which is secreted primarily by the pineal gland of humans and other mammals in response to darkness [24]. It is one of the major and active antioxidants produced in the body and an inverse correlation between progression of breast cancer and melatonin concentrations in blood has been documented [25–28]. In spite of its widely recognized antioxidant role in protecting normal cells against cytotoxicity and apoptosis, melatonin has also been reported to promote ROS generation, leading to cell death in a variety of cancers [29,30]. Unlike its antioxidant properties, signaling pathways and key molecules associated with the pro-oxidant effect of melatonin remain unclear. In the present study, we have explored how melatonin checks breast tumor growth and progression by modulating the redox status, apoptosis, autophagy and inflammation in the tumor vicinity. The study focuses on better understanding the anticancer role of melatonin through regulation of various interlinking pathways which promote tumor progression. Melatonin has been shown to regulate the crosstalk between key signaling cascade to block tumorigenesis. On one hand, melatonin induced amplification of ROS beyond the threshold to interrupt the delicate ROS balance in breast tumor microenvironment, which provides survival advantages to the tumor cells, leading to apoptosis. On the other hand, SIRT 1 upregulation and subsequent downregulation of NF-kB by melatonin mitigates inflammation in breast tumor microenvironment. SIRT 1-induced induction of autophagy through inhibition of PI3K/Akt/mTOR pathway and modulation of NF-kB/pJNK/p53 crosstalk ultimately led to activation of the apoptotic program. Melatonin also modulates the crosstalk between autophagy-inflammation and EMT pathways. Melatonin-induced downregulation of p62 and subsequent reduced expression of Twist 1 and alteration of expression of other EMT marker molecules establishes the fact.

We have established that melatonin-induced tumor regression is associated with activation of SIRT1 and concomitant NF-κB/p65 deregulation. The novelty of this study involves the proposition that melatonin-induced differential modulation of SIRT1 and NF-κB plays a crucial role in the concerted modulation of apoptotic, autophagic and inflammatory pathways in breast cancer.

2. Materials and methods

2.1. Materials

The molecular biology grade reagents utilized in this experiment were all obtained from Sigma-Aldrich Chemical Company (St. Louis, USA), HIMEDIA, and Sisco Research Laboratory (Mumbai, India).

Antibodies: NF-κB (p65) (ab16502), *p*-Akt(Thr 450) (ab108266), PI3K (ab182651), Bcl-2 (ab692), *p*-IκB (Ser 36) (ab133462), SIRT1 (ab110304), SQSTM1/p62 (ab56416), PTEN (ab267787), *p*-mTOR (SerS2448) (ab109268), Twist (ab49254) from abcam (Cambridge, UK); H3B (PA5-22388), beta-actin (MA5-15739), LC3A/LC3B (PA1-16931), p-STAT3 (Tyr705) (MA5-15193), Cleaved caspase 3 (PA5-64749) from ThermoFisher Scientific (Waltham, MA, USA); E-cadherin (610181), Slug (564614), Bax (556467), Ki67 (Alexa Flour 488 tagged) (558616), Beclin1 (612113) from BD Pharmingen (San Jose, CA, USA); Vimentin (sc-373717), alkaline phosphatase-tagged anti-mouse (sc-2358) and anti-rabbit (sc-2008) secondary antibodies were obtained from Santa Cruz Biotechnology Inc. (CA, USA), along with FITC-tagged anti-mouse (sc-2010) secondary antibody. *p*-JNK/SAPK (4668BCE), p-p53 (9281T), p-

STAT3 (9131S) and p53 (9282BCE) from Cell Signaling Technology (MA USA) and STAT3 (137000) from Life Technologies were purchased. The mouse TGF-β, IL-6, TNF-α, and IL-1β ELISA kits were purchased from Ray Biotech (GA, USA). Primers for relevant genes (nf-κb (p65), bax, bcl2, beclin1, p62, atg5, lamp2, sirt1, p53, stat3, il-6 and beta-actin) were designed and synthesized using Primer 3 software genes and reagents related to PCR protocols were acquired from Life Technologies, Thermo Fisher Scientific, USA. HiMedia Laboratories in India was the source of cell culture media and other related items.

2.2. Melatonin (MLT)

Melatonin [Sigma-Aldrich Chemical Company (St. Louis, USA) (M5250); Powder, ≥98 % (TLC)] was dissolved in dimethyl sulfoxide (DMSO) [Sigma-Aldrich Chemical Company (St. Louis, USA)] to prepare 0.2 M (50 mg/ml) stock solution. The stock solution was diluted with PBS to prepare different concentrations of working solution immediately before use.

2.3. Animals

Prior to the experiment, female Swiss albino mice, weighing approximately 25 g and aged between 6 and 8 weeks, were housed in a laboratory for one week after being acquired from licensed animal breeders. The Committee for the Purpose of Control and Supervision on Experiments on Animals (CPCSEA), Ministry of Environment & Forests, New Delhi, India, and the Institutional Animal Ethical Committee (IAEC), Department of Physiology, University of Calcutta (permit number: 820/04/ac/CPCSEA), approved the animal experimentation protocols.

2.4. Isolation and culture of EAC cells

As previously reported by Mukherjee et al., 2021, Ehrlich's Ascites Carcinoma (EAC) cells were maintained by serial intraperitoneal (i.p.) passages of 10^5 cells per mouse, which were obtained from exponentially growing tumors. Mice with tumors in their peritoneum were used to isolate EAC cells. The peritoneal fluid containing tumor cells was removed from the EAC-bearing mice after injecting 2–3 ml of sterile PBS into the cavity. The fluid was then centrifuged for 5 min at 3000 rpm. The cell suspension pellet was used to separate the tumor cells, which were then grown in vitro in RPMI-1640 medium with 10 % FBS, 100 U/ml streptomycin, and 50 U/ml cefotaxim at 37 °C in a CO2 incubator. After a 24-h serum-starvation period, the cells were cultured with progressively higher doses of melatonin (0–10 mM for 0–24 h). For alternate experimental purposes, EAC cells were cultured in presence of H_2O_2 (10 mM) or melatonin (10 mM) with or without *N*-acetyl cysteine (10 mM) for 24 h. Following the designated experimental timeline, the cells and culture media were removed, and centrifuged for 5 min at 3000 rpm. The cells from each group were collected separately and further processing was done [31].

Table 1
Primer SEQUENCE

GENE	PRIMER SEQUENCE (5'→ 3')
IL-6, mRNA	*Forward CTTCCATCCAGTTGCCTT*
	Reverse CCTTCTGTGACTCCAGCTTAT
NF-kB, mRNA	*Forward GAATTCAGTCACTGGCCTCC*
	Reverse TTCAAGACAAAGGAGGTCTGTTT
Stat3, mRNA	*Forward* CCTCCAGGACGACTTTGATTT
	Reverse CCACGAAGGCACTCTTCATTA
Bax, mRNA	*Forward* GCCCTGCCCTTCAGCAT
	Reverse AGCTGCCACATTAGGGTGTCTT
Bcl2, mRNA	*Forward* GTTCTTAAGCCCGATGTGGCAAC
	Reverse GAGTAGTACCAATATGCTACCCTT
P62, mRNA	*Forward* GTGGTGGGAACTCGCTATAAG
	Reverse ATATGGGAGAGGGACTCAAT
Lamp2, mRNA	*Forward* CTGTCTCTTGGGCTGTGAAT
	Reverse GGTGGGAGTTTGGTCTTCTT
Beclin1, mRNA	*Forward* TGTTCCTGTGGAGTGGAATG
	Reverse GGCGTACTCTGGAAACTATCTG
SIRT1, mRNA	*Forward* CCTTGGAGACTGCGATGTTAT
	Reverse GTTACTGCCACAGGAACTAGA
E-cadherin, mRNA	*Forward* AGACTTTGGTGTGGGTCAGG
	Reverse CAGGACCAGGAGAAGAGTGC
Vimentin, mRNA	*Forward* TGGTTGACACCCACTCAAAA
	Reverse GCTTTTGGGGTGTCAGTTGT
P53, mRNA	*Forward* TGCTCACCCTGGCTAAAGTT
	Reverse AGAGGTCTCGTCACGCTCAT
Beta actin, mRNA	*Forward* TGTTACCAACTGGGACGACA
	Reverse GGGGTGTTGAAGGTCTCAAA

2.5. Determination of cell viability

The viability of cultured cells was determined by the 3-(4, 5-dimethylthiazol-2-yl)-2, 5-diphenyltetrazolium bromide (MTT) assay following standard protocol; To the harvested cells (10^6), 200 μl of PBS containing MTT (0.5 mg/ml) was added and incubated for 4 h at 37 °C. After removing the MTT-containing medium, each group received 200 μl of DMSO to dissolve the formazan salt that had formed, and they were then incubated for 10 min. The absorbance was read spectrophotometrically at 540 nm and cell viability was measured as percent of control [31].

2.6. Development of breast tumor model

Isolated EAC cells (~1×10^5 cells) were inoculated into the 4th mammary fat pad of 12 female Swiss albino mice [32,33]. On the 10th day after tumor inoculation, the animals were split up into two groups of six mice apiece: (1) Control (tumor-bearing) Group; injected with 1×10^5 exponentially grown EAC cells on the 4th mammary fat pad; intra-peritoneal injections of PBS + DMSO (vehicle control) from day 10 after tumor inoculation and continued until termination of the experiment, (2) Treated Group; injected with 1×10^5 exponentially grown tumor cells on the 4th mammary fat pad; intra-peritoneal injections for 14 days with melatonin at a dose of 40 mg/kg body weight from day 10 after tumor inoculation and continued until termination of the experiment (Table 1) [34]. Age and sex compatible animals were used as non-tumor control. They received injections of sterile PBS on the 4th mammary fat pad on Day 0. 24 h after the last treatment, the mice were euthanized on Day 25 by intraperitoneal injections (100 mg/kg body weight) of sodium thiopental. Tumor tissues and blood were collected, and different experiments were performed. During the entire experimentation period, all animals were given access to standard diet and drinking water ad libitum until termination of the experiment.

2.7. Estimation of tumor weight and volume

Using a Vernier Caliper, the volume of the isolated tumors was measured and computed using formula $V = 0.5(ab2)$, where "V" stands for the tumor's volume, "a" for its major diameter, and "b" for its minor diameter. Additionally, the weights of individual tumors were determined.

2.8. Cytokine assay

Quantitative measurements of cytokines from tumor tissues (TGF-β, IL-6, TNF-α, and IL-1β) were done using respective ELISA kits according to the manufacturer's protocol. The manufacturer reports that the expected linearity range is 94 % and that the intra- and inter-assay reproducibility is CV < 10 % [35,36].

2.9. Detection of intracellular reactive oxygen species (ROS) content

Both flow cytometric and spectrofluorometric techniques were used to detect intracellular ROS content. For 60 min, 5 μl of whole cell lysates were incubated at 37 °C with 5 mM dihydroethidium present in the media, following which, fluorescent signals were recorded at an excitation wavelength of 480 nm and an emission wavelength of 525 nm in a spectrofluorimeter (JASCO). A standard curve was prepared using increasing concentrations of dihydroethidium (DHE) and the intracellular ROS content were expressed as nanomoles of DHE produced/mg of protein. Intracellular ROS (H_2O_2) was estimated flow cytometrically using 5, 6-chloromethyl-2′7′ dichlorodihydrofluorescien diacetate (CM-DCFDA, Sigma Aldrich, USA). Tumor cells harvested from different experimental groups were incubated with DCFDA solution (25 μg/ml) for 30 min at 37 °C, washed and re-suspended in sterile PBS. ROS content was measured on a flow cytometer (BD FACS VERSE) using the emission intensity of 605 nm. A total of 10,000 events were acquired and analysis was done using FlowJo software (Version 10.7.2) [31].

2.10. Detection of breast tumor cell apoptosis by Annexin V-PI assay

To detect whether melatonin induces apoptosis, live tumor cells (10^6 cells in each case) resected from experimental animals were incubated with PI and Annexin V Fluos (FITC-tagged) (BD Pharmingen, USA) for 15 min at 37 °C. The sample was prepared following the manufacturer's protocol. Excess PI and Annexin V Fluos were then washed off and the cells were analyzed on a flow cytometer (BD FACS Verse, USA). The cells were properly gated for analysis and an electronic compensation of the instrument was done to exclude overlapping of the emission spectra. A total of 10,000 events were acquired and analysis was done using FlowJo software (Version 10.7.2) [36].

2.11. Detection of lysosomal activity linked to autophagy using lysotracker green (LTG) dye

LysoTracker® Green DND-26, purchased from ThermoFisher Scientific, USA, was used to detect autophagy in breast tumor cells. Cell suspensions were made in FACS buffer. It was centrifuged and the pellets were resuspended in pre-warmed Lysotracker green-Propidium iodide (PI) (70 nM working solution) and incubated for 1 h at 37 °C. Next, the cells were washed in PBS and immediately mean fluorescence intensity was obtained on a flow cytometer (BD FACS VERSE) using excitation 504 nm and emission 511 nm. A total of 10,000 events were acquired and analysis was done using FlowJo software (Version 10.7.2) [37,38].

2.12. DAPI staining

For the detection of nuclear fragmentation, tumor cells were fixed in 4 % paraformaldehyde for 15 min; washed twice in cold PBS and permeabilized with 0.2 % Triton X 100. Cells were washed with PBS and nuclear DNA was stained with DAPI (1 mg/ml for 15 min at room temperature). After vigorous washing with PBS to remove excessive stain, cells were mounted and visualized under EVOS M5000 Imaging System (Invitrogen) using UV-filter [35].

2.13. Detection of acidic vesicles by acridine orange staining

Single cell suspensions of tumor cells, prepared from resected breast tumor tissue of the experimental animals, were incubated with acridine orange (Sigma-Aldrich USA) at a concentration of 4 μg/ml for 15 min at 37 °C. Smears were made on slides and the slides were washed repeatedly with PBS at room temperature and immediately observed under EVOS M5000 Imaging System using 450 nm and 593 nm for the detection of acidic vesicular organelles [39,40].

2.14. Hematoxylin eosin staining

For histological studies, breast tumor tissues resected from experimental animals were fixed with 4 % formalin; dehydrated in graded alcohol (50%–100 %) and embedded in paraffin. Thin tissue sections (4–5 μM) were cut. After deparaffinization, the tumor tissue sections were rehydrated with graded alcohol (100, 90, 70 and 50 %). Next the slides were stained with routine hematoxylin eosin stain. Slides were cleaned and mounted with DPX and observed under EVOS M5000 Imaging System [35].

2.15. Immunohistochemistry

Paraffin embedded tissue sections were incubated overnight at 37 °C. They were deparaffinized, rehydrated and immersed in EDTA (1 mM; pH 7.5) for 5 min. Next, for antigen retrieval, the sections were transferred to citrate buffer (10 mM) at 90 °C for 30 min and were then permeabilized with 0.3 % Triton X-100 for 10 min. This was followed by immersion of the sections in H_2O_2 solution (0.3 %) for 5 min and incubation in blocking solution (BSA, 10 %) for 2 h at room temperature. Then the slides were washed thrice in PBST (Tween 20, 0.1 %; in PBS) and incubated with appropriate dilutions of different primary antibodies overnight at 4 °C. The slides were again washed thrice by PBST after which they were incubated with appropriate dilutions of fluorescence-tagged secondary antibodies for 4 h at room temperature and washed again with PBST thrice. All the tissue sections were stained with 1 mM DAPI (in PBS) and incubated at room temperature for 5 min. The slides were washed repeatedly with PBS and mounted and visualized under EVOS M5000 (Invitrogen) Imaging System [35].

2.16. Western blot

In accordance with Gupta et al., 2019, cytosolic, nuclear and whole cell lysates were prepared. For preparing whole cell lysates, isolated breast tumor tissue was homogenized in RIPA buffer following standard protocols. Cytosolic and nuclear fractions were prepared using NE-PER extraction reagents by ThermoFisher Scientific following the manufacturer's protocol [41].

Relevant volumes of nuclear, cytosolic, and cell lysates were loaded onto an SDS-polyacrylamide gel for Western blot analysis. Following electrophoresis, the resolved gel was transferred on to a PVDF membrane in a semi-dry transfer set up. To stop non-specific binding, the membrane was blocked for 1.5 h at room temperature using 3 % bovine serum albumin solution. Appropriate concentrations of particular primary antibodies were incubated on the membrane for an entire night at 4 °C in the blocking solution. Subsequently, the membrane underwent three 15-min washes with TBST (50 mM Tris-HCl, pH 7.6, 150 mM NaCl, and 0.1 % Tween 20) before being incubated for 4 h at room temperature with the appropriate concentrations of particular alkaline phosphatase-conjugated secondary antibodies. To verify equal loading in parallel experiments, a similar quantity of protein was western blotted with the relevant antibodies. H3B was utilized as the nuclear loading control, and beta-actin was used as the cytosolic and whole cell loading controls. The blots were developed using NBT/BCIP (1:1) and the densitometric analyses of the bands were done by using Image J software [31,36].

2.17. mRNA extraction and PCR protocol

RNA extraction and polymerase chain reaction (PCR) were performed following Choudhury et al., 2015. As directed by the manufacturer, total RNA was extracted from the harvested tumor cells using the TRIzol reagent (Ambion RNA, Life Technologies). Using Maxima H Minus Reverse transcriptase 2000 U (ThermoFisher Scientific), 200 ng of the extracted RNA was reverse transcribed to cDNA. Using a premix kit that included DNA polymerase, dNTPs, MgCl2, and buffer (Life Technologies), PCR amplification was carried out in accordance with the manufacturer's instructions. Primers for nf-κb (p65), stat3, il-6, bax, bcl2, beclin1, p62, atg5, lamp2, sirt1, p53, and beta-actin genes were designed and synthesized using Primer 3 software. The primers used for analysis are presented in the table below.

Using agarose gel electrophoresis, the PCR products were resolved, and ethidium bromide staining allowed the bands to be seen. Using Image J software, densitometry of the bands was carried out after the target genes' transcript amounts were normalized to the endogenous reference gene beta-actin [35].

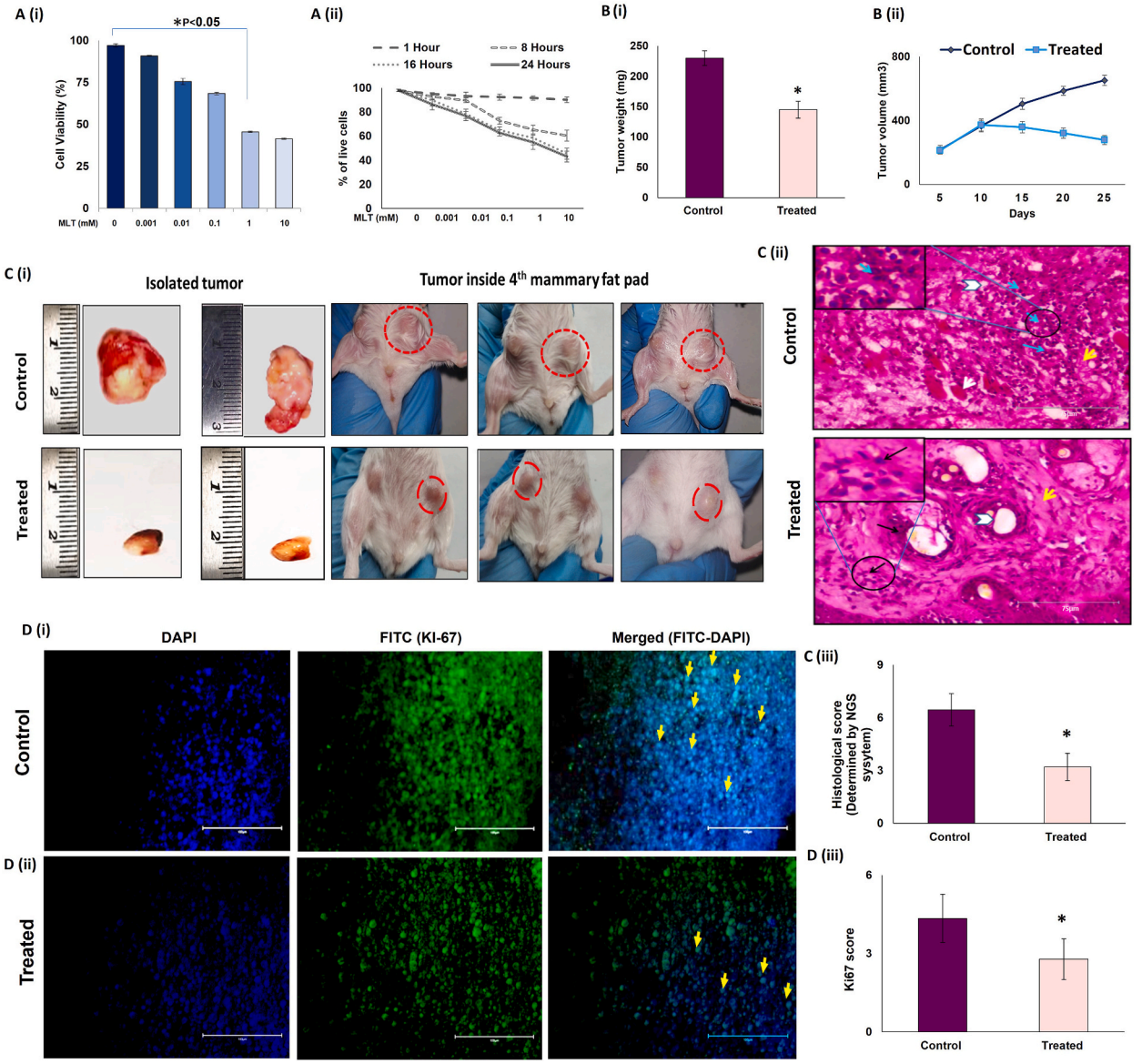

Fig. 1. Melatonin restricts breast tumor growth in female Swiss albino mice A. Dose- and time-dependent inhibition of Ehrlich Ascites Carcinoma cell proliferation by melatonin (MLT). EAC cells were treated with different concentrations (0, 0.001, 0.01, 0.1, 1 and 10 mM) of melatonin and cell viability was assessed by MTT assay at (i) 24-h period and at (ii) different time periods (0, 8, 16 and 24 h). Data represent mean ± S.E.M. of results obtained from three independent experiments. B. Inhibition of in vivo breast tumor growth by melatonin. EAC cells were inoculated in the 4th mammary fat pad of 4–5 weeks old female Swiss albino mice (1×10^5 cells per mouse). Mice were intraperitoneally administered with melatonin at the dose of 40 mg/kg body weight. Significant decreases in (i) tumor weight and (ii) tumor volume in treated groups compared to control. C (i) Representative photographs of primary breast tumor resected from experimental animals 25 days after inoculation of tumor cells in control and treated mice and growth of breast tumors in the mouse orthotopic breast cancer model (Inside 4th mammary fat pad) after consecutive treatments. (ii) Representative histopathology of breast tumors formed within mammary fat pads of Swiss albino mice in control and treated groups. Cancer cells are lined with hyperchromatic nuclei and rarely prominent nucleoli with few mammary gland ducts. Solid pattern with necrosis (white arrow); mammary duct (Arrowhead); tumor cells (Blue Arrows); Inset: Higher magnification of the neoplastic cells with mitosis visible (arrow) and MLT treatment showing tumor regression, clear mammary gland ducts. (iii) Graphs showing histological score in tumor of experimental mice (n = 3). (D) Immunohistochemical (IHC) analysis for Ki67 protein in control and melatonin-treated tumor. (i) Representative photomicrographs of control breast tumor tissue showing high Ki67 positive cells and (ii) melatonin-treated tumor tissue showing low Ki67 positive cells. Columns (from left to right): DAPI-stained nuclei (blue fluorescence); Alexa Flour488-tagged Ki67 antibody (Green fluorescence); merged view of first and second columns. Arrows indicate Ki67 Positive cells. Scale bar 100 μm; Magnification 40X. (iii) Graphical representation of the histological scores (Ki67) in control and melatonin-treated mouse breast tumor tissue (n = 3). Data represent mean ± S.E.M. of results obtained from three independent experiments. *p<0.05; control vs. treated. Refer to Supplementary Material for uncropped images as applicable.

2.18. Statistical analyses

All values were expressed as Mean ± S.E.M., representing triplet of three independent experiments. GraphPad 8.0 (GraphPad Software Inc., CA, USA) software was utilized to identify significant differences between the groups through one-way and two-way analysis of variance (ANOVA). The group means were compared through a two-tailed Student's t-test, with p values less than 0.05 ($p < 0.05$) being deemed significant.

3. Results

3.1. Inhibitory effects of melatonin on breast cancer cell proliferation and viability

To evaluate the effect of melatonin on the viability of EAC cells, MTT assay was performed in vitro by incubating 10^6 EAC cells with 0.0, 0.001, 0.01, 0.1, 1 and 10 mM of Melatonin (MLT) for 0–24 h. We observed a significant decrease in viability of EAC cells both in a dose- [Fig. 1 A (i)] and time-dependent manner [Fig. 1 A (ii)].

To explore the anti-cancer effects of MLT in vivo, we established a breast tumor model by inoculating EAC cells (10^6 cells) in the fourth mammary fat pad of female Swiss albino mice [33] After 9 days of tumor inoculation, the animals of the respective groups were intraperitoneally injected with melatonin for 14 days at a dose of 40 mg/kg body weight [34]. At the end of the experimental period, the animals were euthanized, and the breast tumor tissues were resected. We observed that melatonin treatment significantly regressed tumor growth [Fig. 1 C (i)], as evidenced by marked decrease in tumor weight [Fig. 1 B (i)] and volume [Fig. 1 B (ii)]. Additionally, the decrease in tumor volume in response to MLT treatment was visually evident from the image of the resected tumors isolated from control and melatonin-treated tumor-bearing mice [Fig. 1 C (i)]. MLT-induced tumor regression was also corroborated by histopathological studies of the isolated tumor tissues [Fig. 1 C (ii)]. In the control group, cancerous tissues were lined with hyperchromatic nuclei and rarely prominent nucleoli, few mammary gland ducts, and poorly differentiated structures (blue arrows: tumor cells; yellow arrow: stroma; white arrow: necrosis; white arrowhead: mammary duct). MLT-treated specimens showed tumor regression and clearly differentiated structures like mammary gland ducts [Fig. 1 C (ii)]. Histopathological changes were scored by the NGS system [42,43] which showed that MLT treatment reduced the score by almost 2-fold [Fig. 1 C (iii)]. Tissue sections were stained with Alexa Flour 488 tagged-Ki67, a known marker for cellular proliferation, and its expression is constitutively high in the tumor tissues. We found that MLT treatment significantly reduced Ki67 expression (~67 %), confirming the anti-proliferative action of melatonin in breast tumor [Fig. 1 D (i), (ii) & (iii)].

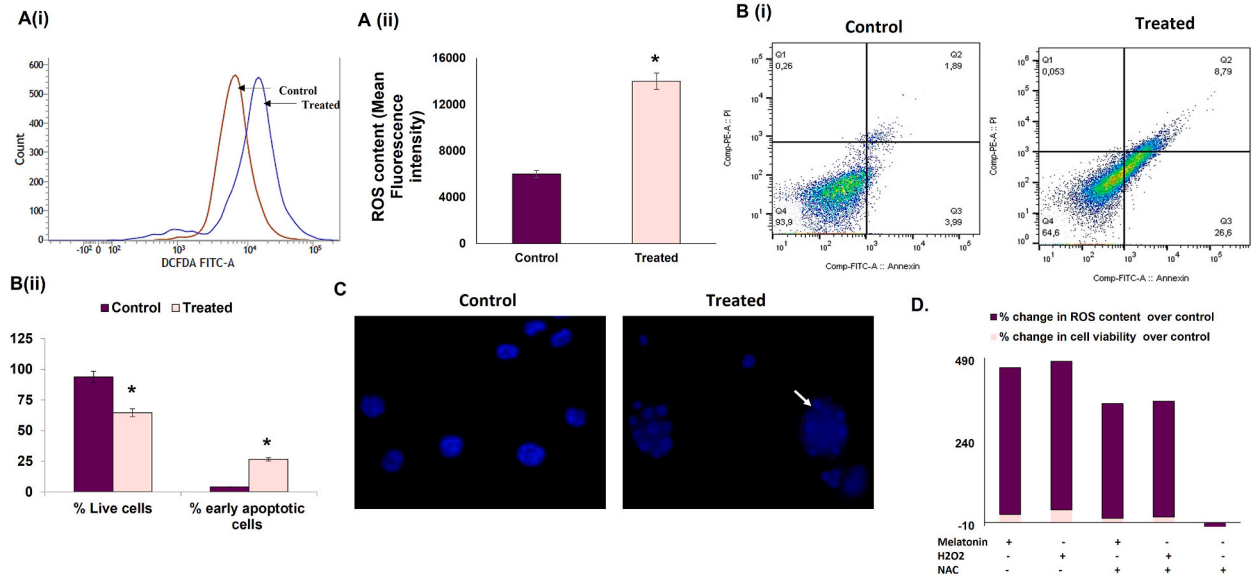

Fig. 2. Melatonin triggers ROS-dependent apoptosis in breast tumor cells. A. ROS generation in breast tumor cells isolated from experimental animals. (i) Histogram showing merged intensities of DCF-DA, (ii) Graphical representation of DCF-DA intensities proportional to the intracellular ROS levels in breast tumor cells isolated from experimental animals analyzed on flow cytometer. B. Melatonin-induced apoptosis of breast tumor cells as analyzed by Annexin V-FITC assay using a flow cytometer. (i) Percentage of apoptotic cells analyzed in control and treated groups and (ii) corresponding graphical representation of percentage of early and late apoptotic cells in control and treated groups. C. Representative images of apoptotic cell death and nuclear morphology in DAPI-stained EAC cells isolated from experimental animals (fluorescence microscopy). White arrow indicates fragmented DNA; magnification: 40X. D. Effect of melatonin on cell death and ROS generation in EAC cells. Spectrofluorimetric detection of ROS and MTT assay for assessment of cell viability of cultured EAC cells under different conditions.

3.2. Melatonin triggers ROS-mediated apoptotic cell death by activating JNK/p53 interaction in breast tumor cells

One of the hallmarks of cancer cells is high intracellular ROS content; the oncogenic nature of which has been well acknowledged, and further increase in the intracellular ROS above the threshold might lead to tumor cell death. We evaluated total intracellular ROS using DCF-DA and found that contrary to its antioxidant role, melatonin treatment in tumor-bearing mice increased ROS in breast tumor cells by more than 2-fold compared to untreated tumor [Fig. 2 A (i) & (ii)].

Increased apoptosis in melatonin-treated breast cancer cells (26.6 % cell death compared to 3.99 % in the control cohort) was established by Annexin-PI assay (flow cytometry) [Fig. 2 B (i) & (ii)]. This observation was supported by fluorescence microscopic images of DAPI staining [Fig. 2 C]. Our studies on the expression of key apoptotic markers (Bax, Bcl-2, etc.) confirmed a pro-apoptotic fate in melatonin-exposed tumor cells as Western blot and PCR studies affirmed an increase in the Bax/Bcl-2 ratio in these cells. [Fig. 3 A & B]. Western blot analysis showed significant increase in cleaved caspase 3 in melatonin-treated group, confirming the execution of apoptosis [Fig. 3 C (i) & (iii)].

To confirm our theory that melatonin-induced breast tumor apoptosis is mediated through excess ROS generation, we performed an *in-vitro* experiment using *N*-acetyl cysteine (NAC) as negative and H_2O_2 as positive control. Incubation of tumor cells with 10 mM NAC decreased ROS content of the cells but did not cause any significant change in the number of dead cells [Fig. 2 D]. Pre-treatment of tumor cells with NAC protected them from the cytotoxic effects of melatonin, because of the ROS scavenging activity of NAC. It can be said that treatment of tumor cells with melatonin significantly increased cell death by increasing ROS generation; indicating that

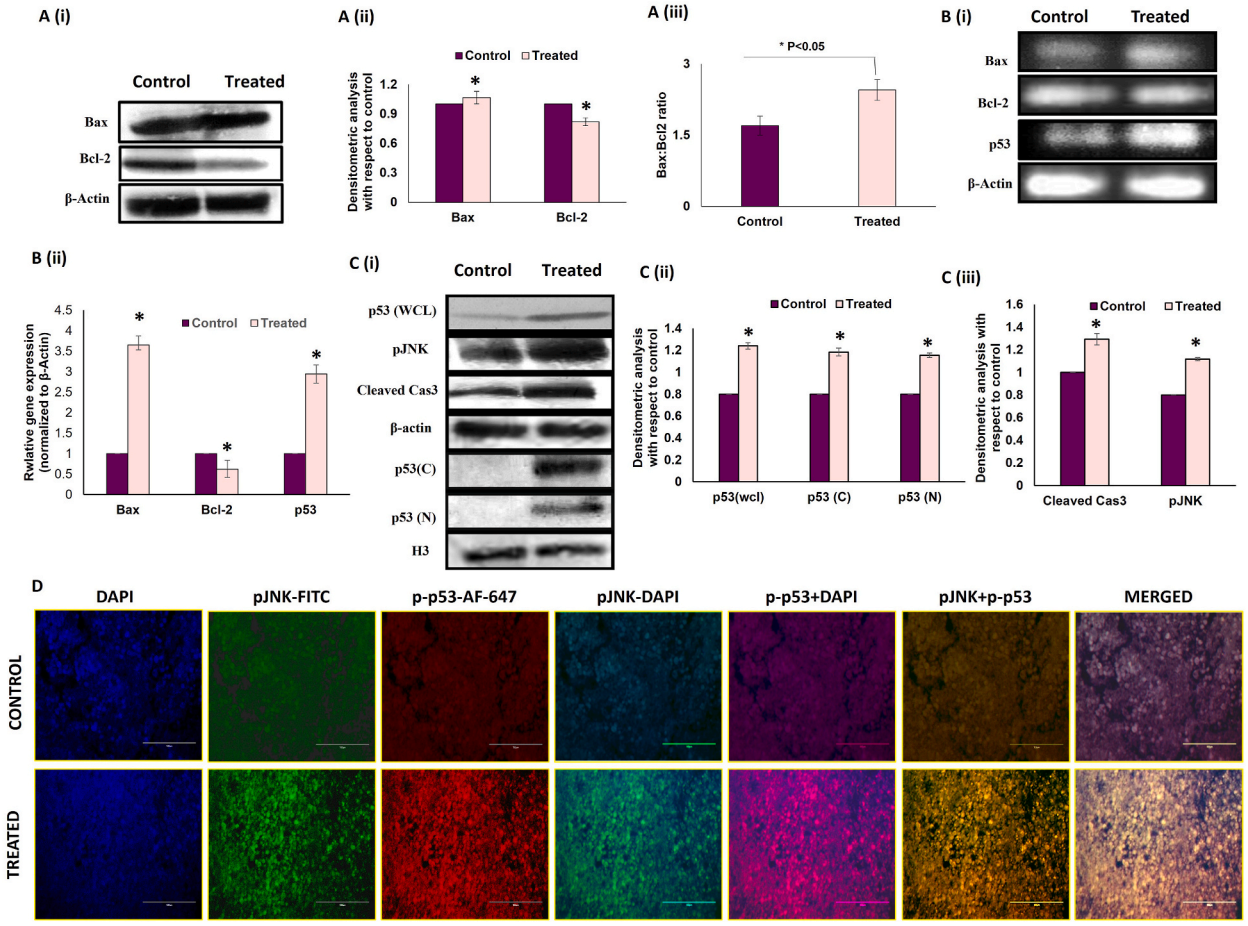

Fig. 3. Melatonin alters the expression of key apoptotic molecules in breast tumor microenvironment. A. Effect of MLT treatment on breast tumor cells isolated from experimental tumor-bearing mice. (i) Western blots and (ii) graphical representation of densitometric analyses of Bax and Bcl2 and (iii) Bax/Bcl2 ratio. B. (i) PCR blot, (ii) graphical representations of densitometric analyses of Bax, Bcl2 mRNA. Beta-actin was used as the loading control for both immunoblotting and PCR. Data are representative of three different blots with similar results. Data represent Mean ± S.E.M. of results obtained from three independent experiments. #p<0.05 between groups. C. Representative (i) immunoblots and (ii) and (iii) densitometric analyses of p53 (wcl; whole cell lysate, C; cytosolic N; nuclear) cleaved caspase 3 and pJNK. D. Representative IHC images showing co-localization of pJNK (FITC; green fluorescence) and p-p53 (AF 647; red fluorescence) counterstained with DAPI, visualized under fluorescent microscope. Expression of pJNK and p-p53 protein in control and melatonin treated tumor. Scale bar: 75 μm; magnification: 40X. Refer to Supplementary Material for uncropped images as applicable.

melatonin induces tumor cell apoptosis by virtue of its pro-oxidant properties.

To further elucidate the molecular mechanisms of ROS-mediated tumor cell death by melatonin, we evaluated the expression of phosphor-Jun *N*-terminal kinases or *p*-JNK, the ROS-activated stress-responsive transcription factor associated with pathways of programmed (apoptosis) and non-programmed (autophagy) signaling [5,44]. Consistent with this, our study showed that melatonin exposure significantly increased the expression of *p*-JNK in the breast tumor compared to non-treated tumor tissue [Fig. 3 C (i) & (iii)].

Also, both the protein and mRNA expressions of the pro-apoptotic p53 were found to be significantly increased in the melatonin-treated group [Fig. 3 C (i) & (ii)]. We confirmed the simultaneous activation of JNK and p53 with immunohistochemistry. Our results demonstrated that melatonin markedly enhanced co-localization of p-p53 and *p*-JNK in melatonin-exposed tumor tissue sections compared to control [Fig. 3 D]. Taken together, these results suggest that melatonin stimulates excess ROS production, which in turn activates ROS-sensitive transcription factors like JNK and p53, leading to activation of apoptotic cell death.

3.3. Melatonin activates the autophagy program in breast tumor cells

Flow cytometric data revealed that treatment of tumor mice with melatonin increased lysosomal acidification (using LysoTracker dye; in presence of melatonin and 1 % H_2O_2 as positive control) in the tumor cells compared to untreated tumor [Fig. 4 A (i) (ii) & (iii)]. The appearance of acridine orange-stained acidic vesicles in the isolated tumor cells confirmed autophagy initiation upon melatonin treatment [Fig. 4 B (i) & (ii)].

To substantiate the role of melatonin in the promotion of autophagy cascade in breast tumor tissue, protein and mRNA expressions of various autophagy markers were investigated [Fig. 5 A & B]. Melatonin-treated tumor group showed marked reduction in p62 (used as a substrate in autophagy) both at protein and mRNA level. Increased protein and mRNA expressions of Beclin1 were also observed [Fig. 5 A (i) & (ii) and B (i) & (ii)]. Additionally, Western blot analysis showed an increase in the LC3BII/I ratio, a well-accepted autophagy marker linked to autophagosome formation [Fig. 5 A (i) & (iii)]. Immunohistochemical analysis of expression of LC3B protein performed in frozen breast tumor tissue sections also showed higher expression of LC3B protein in melatonin-treated tumor

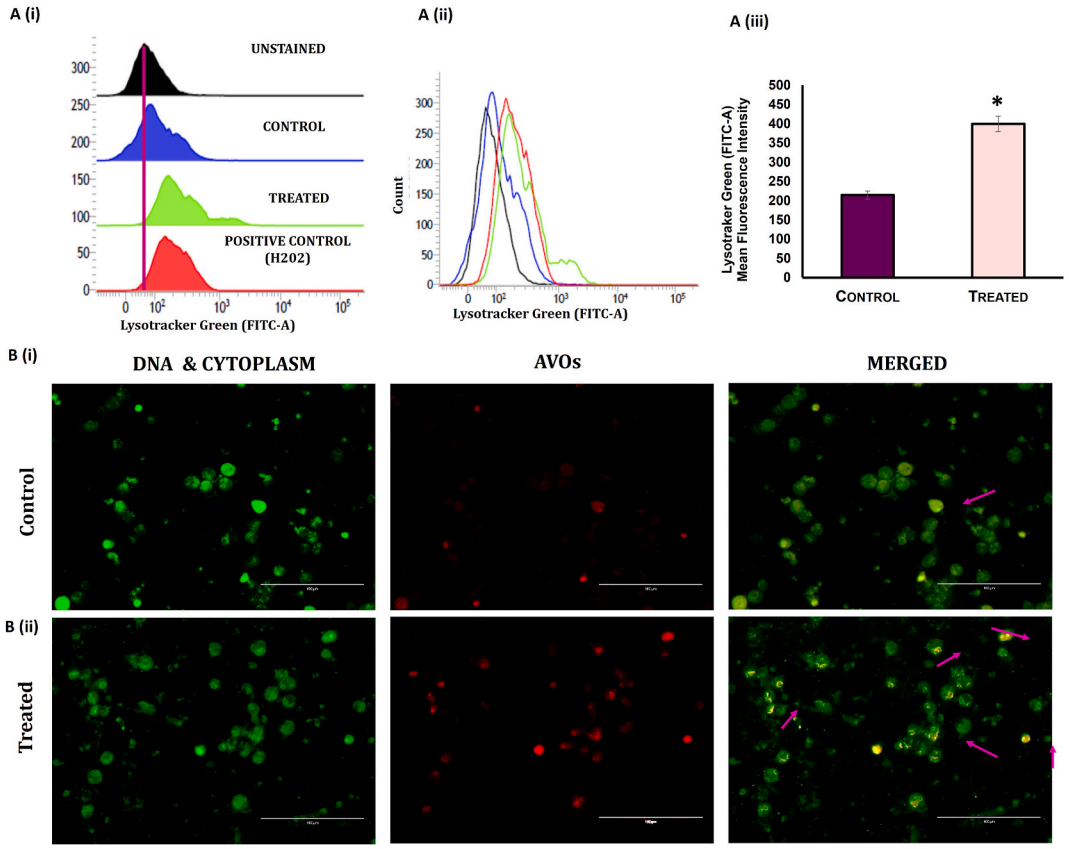

Fig. 4. Melatonin induces autophagy in mouse breast tumor cells. A. Flow cytometric analysis of Lysotracker Dye detection of autophagy in breast tumor cells. (i) and (ii) Histograms showing mean fluorescence intensities of Lysotracker green dye in the breast tumor cells of MLT-treated group compared to control (1 % H_2O_2 was used as positive control). (iii) Graphical representation of mean fluorescence intensities Lysotracker green in different groups. B. Detection of autophagy by acridine orange staining (AO). Cellular autophagy was detected in isolated breast tumor cells (i) control and (ii) treated. Acidic vesicular organelles (AVOs; red fluorescence) as well as cytoplasm and nucleus (green fluorescence) were visualized. Scale bar: 100 μm; magnification: 40X.

specimens compared to control or untreated tumor sections [Fig. 6 C]. From the fluorescence imaging it is quite evident that melatonin induced the expression of LC3B protein in tumor, which indicates more autophagosome formation and increase in autophagy flux. Concomitant increases in Autophagy-related gene 5 (Atg5) expression and decreases in LAMP2 expressions were detected in the melatonin-treated breast tumor cells versus the control tumor cohort [Fig. 5 B (i) & (iii)].

Immunohistochemistry studies on Beclin1 and Bcl-2 co-localization demonstrated an increased Beclin1 versus decreased Bcl-2 expression in melatonin-treated tumor sections. All these results strongly endorse the fact that melatonin instigates both apoptosis and autophagy, which culminate in the death of breast tumor cells and tumor regression [Fig. 5 C].

To substantiate the findings that melatonin increases the autophagy rates, we have performed an *in vitro* experiment in MCF-7 cells using 1 mM melatonin and 5 μm chloroquine concentration for 24h treatment. Higher accumulation of lysosome was observed in Melatonin treated group (iii) compare to control group (i) and Chloroquine treated group (ii) whereas both melatonin and chloroquine treated group (iv) shows reduced accumulation of lysosome compared to group (iii), as detected by lysotracker green dye intensity [Fig. 6 A]. To evaluate the alteration of the expression of key autophagy marker like p62, Beclin1 and LC3B in MCF-7 cells pretreated with melatonin and chloroquine (CQ) in different combination, immunoblotting experiments were performed. Melatonin treated group ($M^{+}C^{-}$) showed reduction in accumulation of p62, substrate of autophagy, whereas chloroquine treated group ($M^{-}C^{+}$) showed higher level of p62 as compared to control group ($M^{-}C^{-}$). CQ treatment ($M^{-}C^{+}$) inhibited Beclin1 expression in MCF-7 cells whereas Melatonin treatment ($M^{+}C^{-}$) increased the expression of Beclin1 which signifies activation of autophagy by melatonin. Increased expression of the LC3 II/I ratio has been observed in melatonin treated MCF-7 cells compared to CQ treated group [Fig. 6 B].

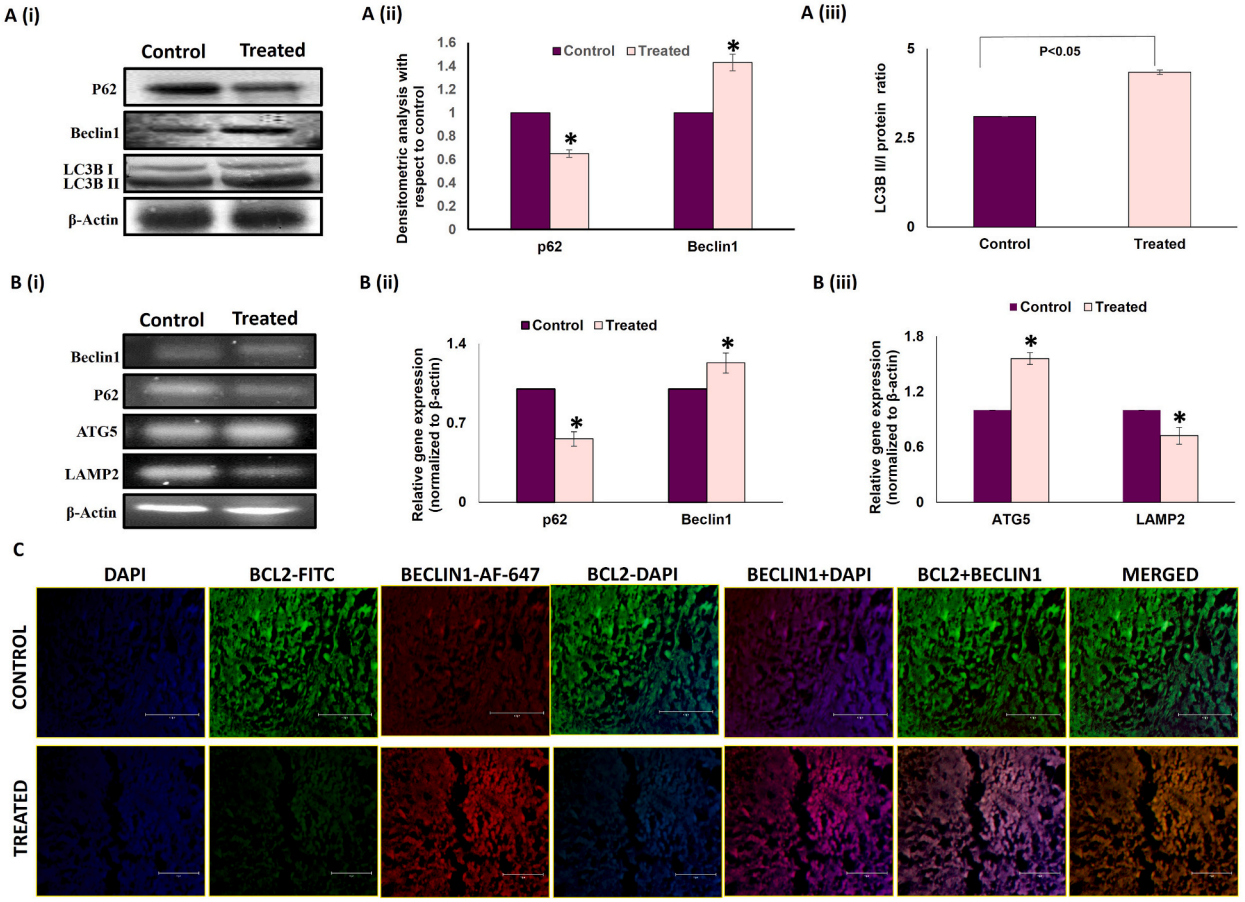

Fig. 5. Melatonin modulates the expression of autophagy regulators in breast tumor. A. (i) Representative immunoblots and graphical representations of expression patterns of (ii) p62 (SQSTM), Beclin1 (iii) LC3B and increased ratio of LC3BII/I in experimental animals. B. (i) Representative gel bands of *Beclin1, p62, ATG5* and *Lamp2* cDNA expressions in control and MLT-treated groups. Densitometric analyses of (ii) *p62*, B*eclin1*, (iii) *ATG5* and *Lamp2* gene in untreated and MLT-treated breast tumor. Beta-actin was used as the loading control in case of both immunoblotting and PCR. Data shown are representative of three different experiments with similar results. Data represented as Mean ± S.E.M. of three separate immunoblots and PCR blots of each experimental group (n = 3). *p<0.05; Control vs. treated. C. Representative IHC images showing co-localization of Bcl2 (FITC; green fluorescence) and Beclin1 (AF 647; red fluorescence) counterstained with DAPI and visualized under standard fluorescent microscope. Scale bar:75 μm; magnification: 40X. Refer to Supplementary Material for uncropped images as applicable.

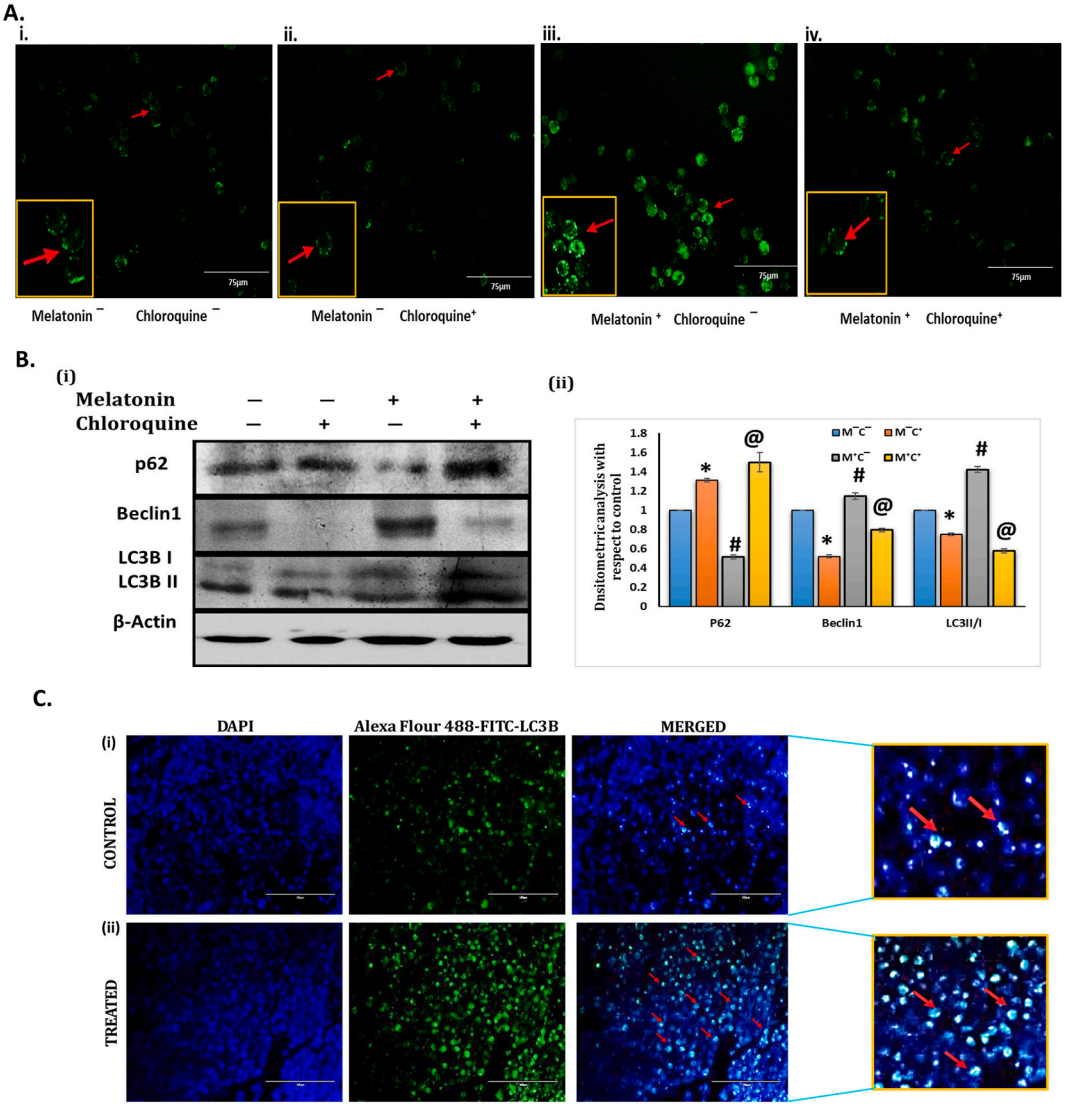

Fig. 6. Activation of autophagy by melatonin in MCF-7 cells *in vitro*. (A) Detection of Autophagy by Lysotracker Green Dye in cultured MCF-7 cells. Representative immunofluorescence detection of lysotracker (Green staning) in MCF-7 cells after 24 h treatment with chloroquine and melatonin in different groups. Fluorescence Microscope was used to visualize the accumulation of lysosomes in terms of intensity of green signal around the nucleus of the cells. (i) Control (no melatonin & chloroquine; **M^-C^-**); (ii) Treated with Chloroquine (5 μm) but no melatonin (**M^-C^+**) (iii) Treated with melatonin (1 mM) but no chloroquine (**M^+C^-**) (iv) Both Melatonin (1 mM) & Chloroquine (5 μm) (**M^+C^+**).Higher accumulation of lysosome was observed in Melatonin treated group (iii) compare to control group (i) and Chloroquine treated group (ii) whereas both melatonin and chloroquine treated group (iv) shows reduced accumulation of lysosome compared to group (iii), as detected by lysotracker green dye intensity. Scale bar 75 μm. (B) (i) Representative immunoblots of p62, Beclin1 and LC3B protein are presented for MCF-7 cells exposed for 24 h treatment with Melatonin (1 mM) & Chloroquine (5 μm) in different experimental groups. (ii) Densitometric analysis of p62, Beclin1 and LC3B II/I ratio. Beta-actin was used as the loading control. Blots shown are representative of three different experiments with similar results. Densitometric data represented as Mean ± S.E.M of three separate immunoblots of each experimental group (n = 3). *p<0.05; Control (**M^-C^-**) vs. **M^-C^+**; #p <0.05; **M^-C^-** vs. **M^+C^-** and @ p <0.05; **M^-C^-** vs. **M^+C^+**. Control (no melatonin & chloroquine; **M^-C^-**); Treated with Chloroquine (5 μm) but no melatonin (**M^-C^+**); Treated with melatonin (1 mM) but no chloroquine (**M^+C^-**); Both Melatonin (1 mM) & Chloroquine (5 μm) (**M^+C^+**). **(**C) Immunohistochemical analysis of expression of LC3B protein performed in frozen breast tumor tissue sections. **(i)** Representative IHC images showing lower expression of LC3B protein (green fluorescence) in control tumor section and (ii) higher LC3B expression in melatonin-treated tumor tissue sections as revealed by standard fluorescent microscopy**. (Red arrow** indicates the expression of LC3B Protein). Refer to Supplementary Material for uncropped images as applicable.

3.4. Melatonin subdues the pro-inflammatory bias in the breast tumor microenvironment by modulating the IL-6/STAT3/NF-κB p65 axis

It is well-established that a pro-inflammatory bias in the tumor microenvironment accelerates tumor growth and survival [10]. From our studies, it was quite evident that a strong pro-inflammatory tumor microenvironment developed around the breast tumor tissue due to significant increase in pro-inflammatory cytokines IL-6, TNF-α and IL-1β as compared to non-tumor breast tissue [Fig. 7 A]. Melatonin treatment led to marked decrease in these cytokines, indicating a reduced inflammatory setting in the tumor microenvironment [Fig. 7 A]. Besides, melatonin exposure also significantly reduced the level of tumorigenic pro-survival cytokine TGF-β [Fig. 7 A].

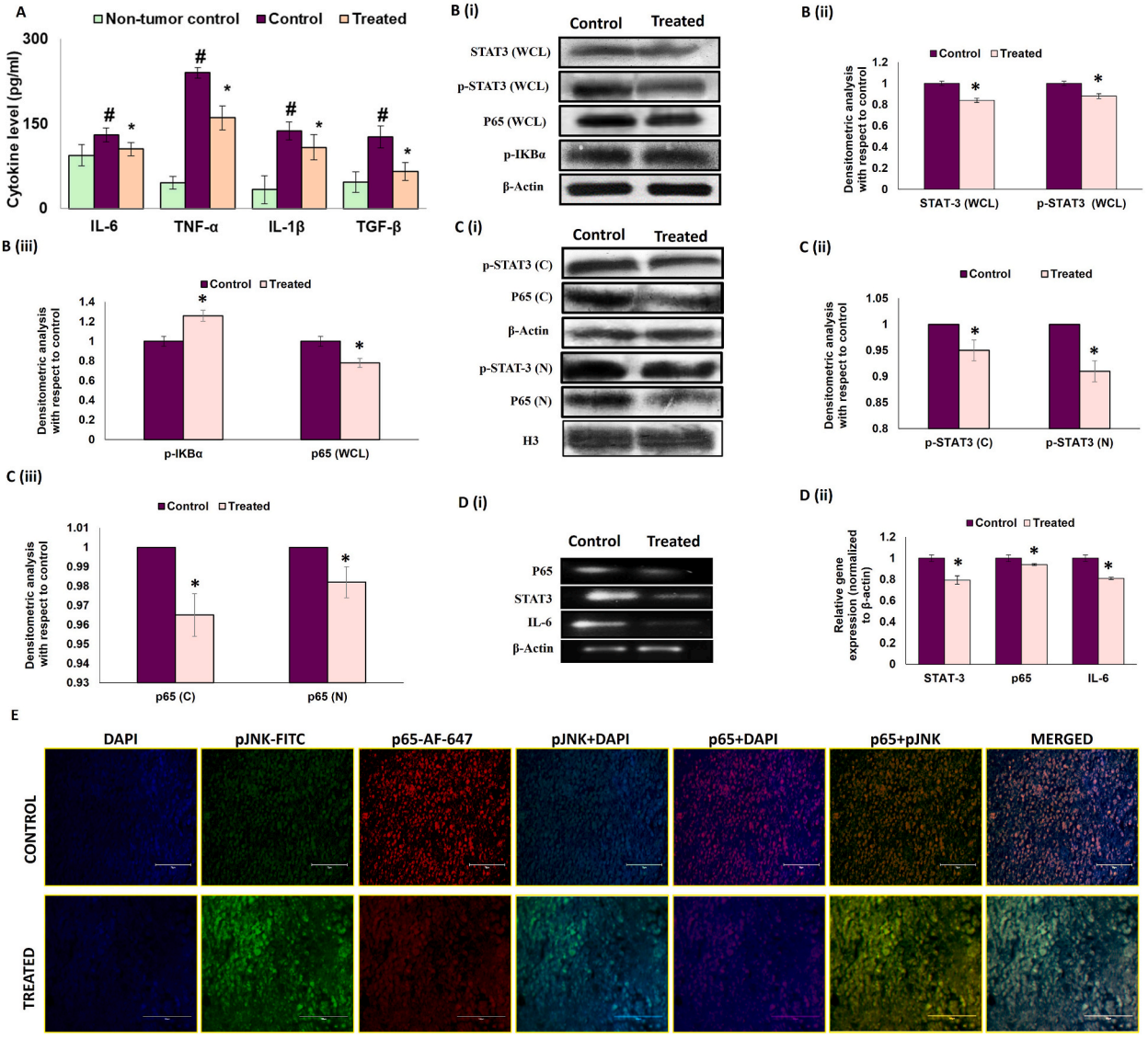

Fig. 7. Melatonin reduces the pro-inflammatory bias in the breast tumor microenvironment. A. Expression of various cytokines (IL-6, IL-1β, and TNF-α, TGF-β) in breast tumor microenvironment. B. (i) Representative immunoblots and graphical representation of densitometric analyses of expression patterns of (ii) STAT3 (whole cell lysate), p-STAT3 (whole cell lysate), (iii) *p*-IκBα and p65 (whole cell lysate). C. Nuclear translocation of p-STAT3 and p65. (i) Representative immunoblots and graphical representation of expression patterns of (ii) p-STAT3 (cytosolic lysate), p-STAT3 (nuclear lysate), (iii) p65 (cytosolic lysate) and p65 (nuclear lysate). D. (i) Representative PCR blots and graphical representation of gene expression patterns of (ii) *p65*, *stat3* and *il-6*. Beta-actin was used as loading control in case of both immunoblotting (for whole cell and cytosolic lysates) and PCR and H3 was used as the loading control in case of nuclear lysate. Immunoblot and PCR blots shown here are representative of three different blots with similar results. Densitometric data represented as Mean ± S.E.M of three separate immunoblot and PCR blots of each experimental groups (n = 3). #p<0.05; tumor control vs. MLT treated tumor groups. E. Immunohistochemical (IHC) analysis of co-localization of *p*-JNK (FITC; green fluorescence) and NF-κB p65 (AF-647; red fluorescence) counterstained with DAPI & visualized under fluorescent microscope. Scale bar present: 100 μm; magnification: 40X. Refer to Supplementary Material for uncropped images as applicable.

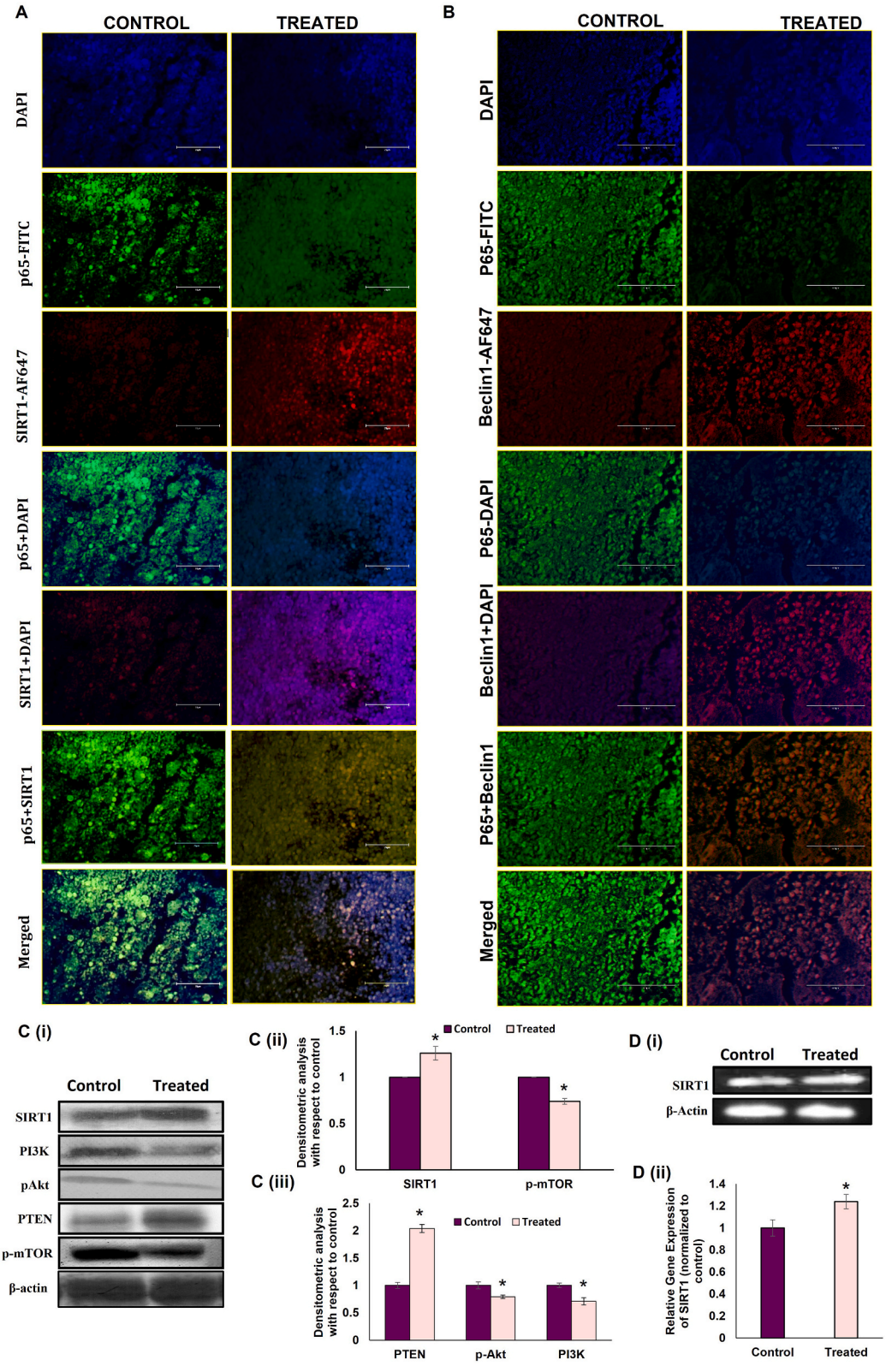

(caption on next page)

Fig. 8. Melatonin modulates SIRT1/PI3K/Akt/mTOR/Beclin1 expressions in breast tumor cells. A. Representative IHC images showing co-localization of (A) p65 (FITC; green fluorescence) and SIRT1 (AF-647; red fluorescence) counterstained with DAPI & visualized under standard fluorescent microscope. (B) NF-κB (FITC; green fluorescence) and Beclin1(AF 647; red fluorescence) counterstained with DAPI & visualized under fluorescent microscope. Scale bar:100 μm; magnification 40X. C. (i) Representative immunoblots and (ii) and (iii) graphical representations of gene expression patterns of SIRT1, *p*-mTOR and PTEN, PI3K and *p*-Akt. D(i) Representative PCR blot and (ii) graphical representation of SIRT1 gene. Beta-actin was used as the loading control. Blots shown are representative of three different experiments with similar results. Densitometric data represented as Mean ± S.E.M of three separate immunoblot and PCR blots of each experimental group (n = 3). *p<0.05; tumor control vs. MLT treated tumor groups. Refer to Supplementary Material for uncropped images as applicable.

In order to investigate the plausible molecular basis for the pro-inflammatory bias in the tumor microenvironment and the mechanism by which melatonin mitigates this response, we theorized that there might be involvement of a signaling pathway regulated by JNK, NF-κB/p65 and STAT3; key transcription factors that are known to promote cell survival by modulating a diverse array of cytokines in response to inflammatory stress [45–47].

The unique pro-apoptotic and anti-inflammatory activity of melatonin in the tumor microenvironment was clearly illustrated by our immunohistochemistry study of *p*-JNK and NF-κB/p65. Results showed that melatonin noticeably inhibited the expression of p65 and at the same time upregulated *p*-JNK expression in tumor tissue [Fig. 7 E]. Further, Western blot analysis followed by fluorescence microscopy clearly revealed that melatonin blocked the nuclear translocation of NF-κB/p65, which resulted in reduced IL-6 expression [Fig. 7B and C]. IL-6 is known to facilitate phosphorylation/activation of STAT3. A decrease in IL-6 upon melatonin treatment led to simultaneous reduction in protein and mRNA expressions of activated p-STAT3 [Fig. 7 B, C & D]. Blockade of the NF-κB-p65/IL-6/STAT3 axis upon melatonin treatment created an anti-inflammatory bias in the breast tumor microenvironment.

3.5. Melatonin-induced anti-inflammatory responses instigate autophagy in the tumor microenvironment by interrupting NF-κB/SIRT1 and NF-κB/Beclin1 interactions

From our data, it has been made quite clear that melatonin reverses the pro-inflammatory bias in the tumor microenvironment. We speculated that autophagy activation might be the pivotal factor responsible for melatonin-induced anti-inflammatory responses in the tumor microenvironment. SIRT1 is a known histone deacetylase that plays central role in various cellular signaling pathways such as inflammation, apoptosis, and autophagy [48,49] by regulating transcription factors such as p53, FOXO and NF-κB. In case of autophagy, SIRT1 positively regulates several autophagic genes like Atg5 and Atg 8 by means of deacetylation [50,51]. To establish the direct role of autophagy in reducing inflammation in the tumor microenvironment, we checked for NF-κB/SIRT1 and NF-κB/Beclin1 interactions by immunohistochemistry. Results indicated that melatonin substantially inhibited NF-κB expression in SIRT1 as well as Beclin1-positive cells in tumor tissue, compared to untreated tumors [Fig. 8 A & 5 B]. Our hypothesis was further confirmed by significant increases in both protein and gene expressions of SIRT1 by 1.35 fold and 1.29 fold respectively [Fig. 8 C & 5 D]. To confirm the pro-autophagic role of SIRT1, we then observed the expression of the components of PI3K/Akt/mTOR pathway which is known to downregulate the autophagy program [19,22]. Western blot analyses showed that melatonin decreased p-PI3K expressions in breast tumor cells by ~40 % [Fig. 8 C (i) & (iii)]. Consequently, phosphorylation of Akt and mTOR was also inhibited, as evident from Western blot analyses of *p*-Akt and *p*-mTOR in the breast tumor cells of melatonin-treated mice [Fig. 8 C (i) & (ii) & (iii)]. We also found an increase (19.35 %) in the expression of PTEN, the negative regulator of PI3K/Akt, in breast tumor tissue of melatonin-exposed experimental mice [Fig. 8 C (i) & (iii)].

3.6. The pro-autophagic and anti-inflammatory responses initiated by melatonin in the tumor microenvironment inhibits EMT in breast tumor cells

It is now understood that exaggerated inflammatory responses in the tumor microenvironment potentiates tumorigenesis [52] and, at the same time, inhibition of stress-responsive autophagic cell death induces tumor cell survival [53,54]. For the next phase, our aim was to evaluate whether activation of inflammation and inhibition of autophagy instigates epithelial to mesenchymal transition in breast tumor cells and whether melatonin treatment could mitigate this pro-tumorigenic response. Our Western blot data implied that there was significant induction of mesenchymal markers, such as, Vimentin, Slug, Twist and MMP-9, with subsequent decrease in epithelial marker, E-cadherin in the breast tumor cells. Melatonin treatment reversed these protein expression patterns [Fig. 9 C (i) & (ii) & (iii)]. We also evaluated the mRNA expressions of E-cadherin, Vimentin, Slug and Twist [Fig. 9 D (i), (ii) & (iii)] and obtained similar results.

We performed co-localization studies for NF-κB and Slug (a mesenchymal marker) and found that co-localization of both these proteins were notably inhibited by melatonin treatment in breast tumor [Fig. 9 A]. Co-localization analyses for p62 and Twist1 have revealed that higher accumulation of p62 in control tumor is associated with stabilization of Twist1 whereas melatonin treatment significantly inhibited the expression of both these proteins [Fig. 9 B].

Our experimental results verified that melatonin inhibits epithelial to mesenchymal transition in breast tumor tissues; thereby supporting its anti-metastatic potential and validated our hypothesis that melatonin mitigates tumorigenesis through its anti-inflammatory and pro-autophagic responses.

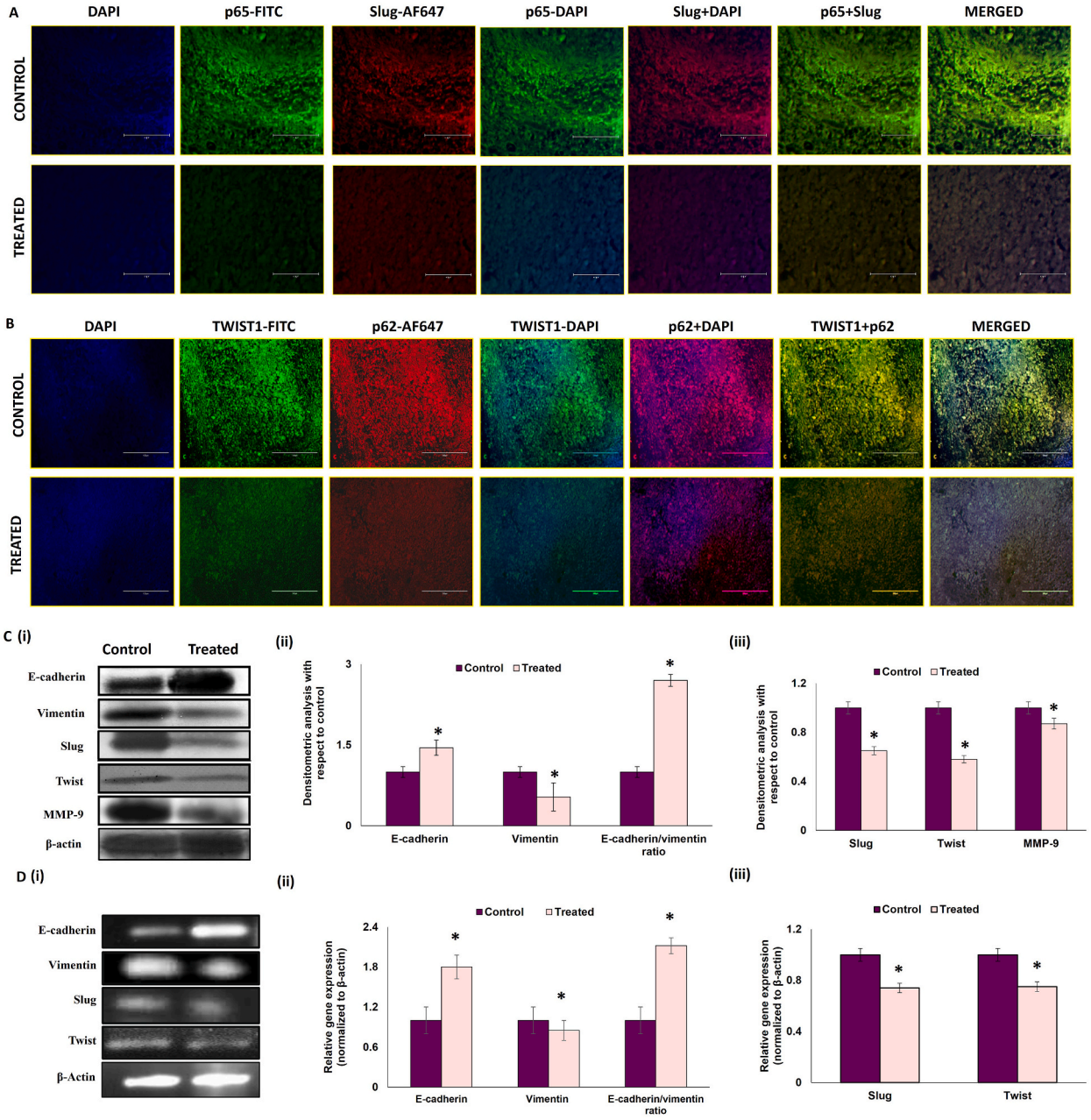

Fig. 9. Melatonin modulates the expression of EMT proteins in breast tumor Representative IHC images showing co-localization of A. p65-NF-κB (green fluorescence) and Slug (red fluorescence) and B. Twist1 (green fluorescence) and p62 (red fluorescence) counterstained with DAPI & visualized under fluorescent microscope. Scale bar: A75 μm and B 100 μm; magnification: 40X. C. (i) Representative immunoblots and (ii) and (iii) graphical representations of expression patterns of E-cadherin, Vimentin, Slug, Twist and MMP-9 proteins. D (i) Representative PCR blots and (ii) and (iii) graphical representations of gene expression patterns of *e-cadherin*, *vimentin, slug* and *twist*. Beta-actin was used as loading control in case of both immunoblotting and PCR. Immunoblot and PCR blots shown here are representative of three different blots with similar results. Densitometric data represented as Mean ± S.E.M. of three separate immunoblot and PCR blots of each experimental groups (n = 3). '*' Represents significant difference with respect to control at $p<0.01$. Refer to Supplementary Material for uncropped images as applicable.

4. Discussions

There is evidence that melatonin might enhance the efficacy of certain chemotherapy drugs and reduce their side effects. Melatonin might be used as an adjunct to conventional cancer treatments like chemotherapy or radiation therapy. It is thought that melatonin's antioxidant properties could help protect healthy cells from the damage caused by chemotherapy or radiation, while also increasing

the sensitivity of cancer cells to treatment. However, the timing and dosage of melatonin administration in relation to these treatments would need to be carefully considered to avoid interference. Cancer treatments like chemotherapy and radiation often cause significant side effects, including fatigue, insomnia, and cognitive impairment. Melatonin's role in regulating sleep might help alleviate some of these symptoms and improve the overall quality of life for cancer patients. In recent years, melatonin has gained recognition as a valuable adjuvant to traditional anticancer therapies [55,56]. Clinical studies investigating the combined use of melatonin and chemotherapy drugs have demonstrated its potential to mitigate drug-induced side effects, yielding positive outcomes for cancer patients [57]. Melatonin's ability to sensitize cancer cells to chemotherapy-induced apoptosis and autophagy has also been documented [58–60]. Notably, randomized clinical trials involving patients with head and neck cancer revealed that co-administration of melatonin inhibited patients' antioxidant capacity, resulting in reduced pain and mucositis [61]. Furthermore, the combination of cisplatin and melatonin exhibited promising results in addressing common side effects such as anemia.

In the context of metastatic colorectal cancer, a notable development emerged in the form of a combination therapy involving subcutaneous IL-2 and melatonin as a second-line treatment subsequent to the use of 5-FU in the first-line therapy. This novel approach showcased improved survival rates. Recent investigations have also highlighted the synergistic potential of melatonin and doxorubicin in augmenting apoptosis and autophagy within human breast cancer cells. This effect was attributed to a reduction in the AMPKα transcription factor [62].

Application of chemotherapeutic drugs has its own limitations in the form of side-effects, impacting organs of the body. Anticancer therapeutics with standard safety profile and well-established clinical settings is ideal for treatment of cancer. Melatonin has been used as an adjuvant with different chemotherapeutic drugs for treating different types of cancer at different phases. Nonetheless, melatonin has some limitations as an anticancer drug.

A potential limitation is very short half-life (approx. 45 min) of melatonin by both oral and intravenous routes and low oral bioavailability [63]. Uncertain administration approaches make melatonin less efficacious in treating cancer. Low water solubility and low shelf life is also a barrier in therapeutic application of melatonin. Low biocompatibility of melatonin is also an issue. There is no uniform dosing regimen for use of melatonin in treating cancer in initiation, promotion and progression phases. Uncertain therapeutic doses and side-effects of melatonin on cancer patients warrants more study to evaluate the optimum uniform dosage of melatonin for its better application in clinical trials [64]. Understanding the molecular mechanisms and crosstalks would provide better insights for its optimum applications as an anticancer agent. Our study was designed with the same purpose and will facilitate the better understanding of melatonin as an anticancer agent.

We investigated the molecular basis for the anti-tumor activities of melatonin with special reference to modulation of the signaling pathways, dialogues, and cross talks in breast tumor microenvironment. Melatonin suppressed tumor viability in vitro in a dose- and time-dependent manner [Fig. 1 A (i) and (ii)] and melatonin treatment (40 mg/kg for 14 days) significantly reduced tumor weight, volume, and size in our in vivo model of mouse breast tumor [Fig. 1 B (i) & (ii) & C (i)]. Immunohistochemical analysis of Ki67 is routinely done to monitor proliferative activity of cancer cells and treatment responses. We observed that melatonin treatment was associated with a decrease in Ki67 indicating marked reduction in tumor cell proliferation [Fig. 1 D (i) & (ii)].

In vitro studies on MCF-7 and MDA-MB-231 cancer cell lines have shown that melatonin induced apoptosis by regulating the relative expressions of pro- and anti-apoptotic proteins [65]. Our data also showed skewed Bax/Bcl-2 ratio in favor of apoptosis in response to melatonin [Fig. 3 A & B]. Our flow cytometric data confirmed that melatonin treatment led to a significant increase in early apoptotic cell populations in breast tumor (Annexin V-FITC/PI assay). In an interesting turn, our next set of data showed that breast tumor cell death upon treatment with melatonin, the known antioxidant, was associated with marked increase in intracellular ROS [Fig. 2 A (i) & (ii)]. High level of intracellular ROS leads to deacetylation of p53 by SIRT1 (a class III histone deacetylase), blocking its nuclear translocation and subsequent cytosolic accumulation, which ultimately results in transcription-independent p53-induced apoptosis [56,66,67].

The ubiquitous transcription factor NF-κB has been reported to act as an anti-apoptotic molecule through the downregulation of JNK, by suppressing the build-up of ROS [11,12,68]. Our results show that melatonin treatment significantly altered the expression pattern of both the markers with decreased NF-κB and increased *p*-JNK, which would signify that melatonin-induced downregulation of NF-κB/p65 is associated with ROS accumulation and JNK activation which triggers breast tumor cell apoptosis [Fig. 7 E].

The tumor microenvironment (TME) is characterized by persistent inflammation and the most critical inflammatory marker that is upregulated in almost all cancer cells is NF-κB [69]. In our model, the presence of an inflammatory milieu in the TME was evident from increased expressions of NF-κB/p65, p-STAT3 and inflammatory cytokines IL-6, IL-1β and TNF-α. Several studies have correlated high levels of IL-6 with bad disease prognosis in cancer patients [45]. IL-6 is known to promote the phosphorylation and activation of STAT3 which is responsible for mediating inflammatory responses [70]. Studies showed that STAT3 essentially participates in numerous cellular events in cancer cells including cell proliferation, metastasis and EMT [16,71–73]. Activated STAT3 dimerizes and translocates to cell nucleus and directly binds to the specific promotor region of targets, such as Bcl-2 families, MMP-2, MMP-9 and Vimentin, leading to their transcriptional activation [14,15]. Recent studies have shown that suppression of phosphorylated STAT3 can induce apoptosis and inhibit metastasis in cancer cells [74]. There are reports on the role of IL-6/STAT3/NF-κB feedback loop in breast cancer progression through IL-6 mediated persistent activation of breast stromal fibroblasts [75]. In our study, melatonin treatment was found to significantly subdue the inflammatory cytokines in the breast tumor microenvironment [Fig. 7 A]. There was a high level of basal p-STAT3 in the tumor cells and melatonin efficiently blocked STAT3 phosphorylation as well as nuclear translocation of p-STAT3. We also observed significantly reduced nuclear presence of NF-κB compared to the cytosol [Fig. 7 B & C].

A persistent inflammatory state, as seen in the breast tumor microenvironment, can block the induction of autophagy [70]. To corroborate the above notion, we analyzed the expression patterns of key molecular players of the autophagy pathway. In our experiments autophagosome formation upon melatonin treatment was confirmed by Lysotracker staining [Fig. 4 A (i), (ii) & (iii)]. When

visualized under a fluorescence microscope, acidic vesicular organelles (AVOs) of the acridine orange-stained melatonin-treated breast tumor cells appeared as distinct dot-like structures distributed within the cytoplasm or localized in the perinuclear regions [Fig. 4 B (i) & (ii)]. Melatonin was also shown to modulate various autophagy factors including Beclin1, p62, Atg5, Lamp2 and autophagy-related protein microtubule-associated protein 1 light chain 3 (LC3).

The interplay between the anti-apoptotic protein, Bcl-2, and the autophagy protein, Beclin1, marks the point of convergence of apoptotic and autophagic pathways. Bcl-2 proteins bind to Beclin1 and disrupt its autophagy function. In the absence of Bcl-2 binding, Beclin1 induces autophagy and promotes cell death [76,77]. To validate whether melatonin has any role in modulating Bcl-2/Beclin1 interaction and activation of autophagy as shown in previous results, co-localization experiments were performed to analyze the expressions of both the molecules. Results showed higher expression of Bcl-2 and lower expression of Beclin1 in control tumor while melatonin treatment reversed this pattern of expression [Fig. 5 C], endorsing the pro-autophagic and pro-apoptotic role of melatonin in breast tumor. In vitro experiment in MCF-7 cells treated with melatonin and chloroquine in different combination showed higher intensity of lysotracker green staining [Fig. 6A] and increased level of beclin1 and LC3B II/I ratio [Fig. 6 B] in melatonin treated group compared to control and chloroquine treated group, indicates melatonin induced activation of autophagy in MCF-7 breast tumor cells.

The tumor suppressor phosphatase and tensin homolog (PTEN) proteins are negative regulators of the PI3K pathway, and have pro-autophagic activities [22]. Kma et al., 2022 reported that increase in intracellular ROS in response to flavonoids in non-small cell lung cancer cell line corresponded with higher PTEN and lowered Akt levels leading to a higher occurrence of autophagy [68,78]. The PI3K/Akt/mTOR pathway is frequently activated in cancer cells, promoting malignant transformation and apoptosis resistance; and is an important axis to target for drug development [19,20]. Our data showed an increased expression of PTEN and decreased levels of phosphorylated Akt in melatonin-exposed breast cancer cells [Fig. 8 C (i) & (iii)]. In the present scenario, melatonin-induced reduced phosphorylation of Akt led to decreased phosphorylation of mTOR [Fig. 8 C (i), (ii) & (iii)] and consequently, activation of autophagic pathways in melatonin-exposed breast tumor tissue. Additionally, as PI3K/Akt are survival inducers, their inhibition blocked cell survival and triggered apoptosis.

Decreased sirtuin 1 (SIRT1) expression is associated with enhanced NF-κB-dependent inflammation and compromised autophagic responses [79]. Accumulating evidence indicates an autophagy suppressive role of NF-κB through inhibition of Beclin1 [80]. Our Western blot, gene expression and immunohistochemistry data established higher SIRT1 protein expression in melatonin-treated tumor group [Fig. 8 C (i), (ii) & D (i) (ii)]; whereas, there was significant reduction in NF-κB expression [Fig. 7 C]. Further, NF-κB/SIRT1 and NF-κB/Beclin1 co-localization studies [Fig. 8 A and B] pointed towards a reduced NF-κB expression in SIRT1 as well as Beclin1-positive cells in melatonin-treated tumor tissues. From these results it is evident that melatonin-induced anti-inflammatory responses instigate autophagy in the tumor microenvironment by modulating the NF-κB/SIRT1 and NF-κB/Beclin1 interactions.

Tumor cells undergo a phenotype switch during epithelial to mesenchymal transition (EMT), losing their epithelial features and acquiring mesenchymal phenotype leading to increased invasiveness. This process is reversible and regulated mostly by the transcription factors such as, Snail, Slug and Twist1 [81,82]. Our data indicated that melatonin regulates some of the key proteins related to EMT. Melatonin induced upregulation of E-cadherin and downregulation of Vimentin, Slug and Twist1 both at protein and mRNA levels was observed [Fig. 9 C, D]. These data point strongly towards an anti-EMT potential of melatonin.

Studies have shown correlation between enhanced p62 activity with tumorigenesis and impaired or inefficient autophagy and NF-κB activation [83–86]. Several reports have established that p62 accumulation leads to EMT progression via Twist1 stabilization and decreased E-cadherin expression [87]. Co-localization studies of p62 (SQSTM1) & Twist1 have revealed higher expression of both p62 and Twist1 in control tumor group and treatment with melatonin reversed these changes [Fig. 9 B]. Activated NF-κB upregulates transcriptional activation of EMT-related gene expressions in human breast cancer via direct association to the EMT transcription factors (Snail 1, Slug and Twist1) promoter sites [88]. Co-localization studies of NF-κB and Slug proved simultaneous downregulation of both the proteins in melatonin-treated tumor samples [Fig. 9A]. Our findings suggest that melatonin prevents EMT progression in breast tumor cells by activating autophagy and anti-inflammatory responses, altering the interactions between p62/Twist1 and NF-κB/Slug proteins.

5. Conclusion

Based on above findings, we can conclude that modulation of interactions among key molecules at the hub of tumorigenesis; like, SIRT1-NF-κB, p62-Twist1, and NF-κB-Slug, is responsible for the establishment of a pro-death apoptotic and autophagic fate in melatonin-exposed breast cancer cells.

Data Availability Statement

Data associated with this study has not been deposited into any publicly available repository due to the novel and sensitive nature of the data. Data will be made available on request.

CRediT authorship contribution statement

Nirmal Das: Writing - review & editing, Writing - original draft, Validation, Methodology, Investigation. **Sudeshna Mukherjee:** Writing - review & editing, Methodology, Investigation. **Ankur Das:** Writing - review & editing, Validation, Methodology, Investigation. **Payal Gupta:** Writing - review & editing, Validation, Methodology. **Amit Bandyopadhyay:** Writing - review & editing, Resources. **Sreya Chattopadhyay:** Writing - review & editing, Visualization, Validation, Supervision, Project administration,

Investigation, Formal analysis, Conceptualization.

Declaration of competing interest

The authors declare that they have no known competing financial interests or personal relationships that could have appeared to influence the work reported in this paper.

Acknowledgements

The authors acknowledge CSIR, DST-INSPIRE, DST-SERB, Government of India for fellowship support. The authors also acknowledge infra-structural support of the Centre for Research in Nanoscience and Nanotechnology (CRNN), University of Calcutta.

References

[1] B. Perillo, M. Di Donato, A. Pezone, E. Di Zazzo, P. Giovannelli, G. Galasso, G. Castoria, A. Migliaccio, ROS in cancer therapy: the bright side of the moon, Exp. Mol. Med. 52 (2) (2020 Feb) 192–203, https://doi.org/10.1038/s12276-020-0384-2.
[2] S. Galadari, A. Rahman, S. Pallichankandy, F. Thayyullathil, Reactive oxygen species and cancer paradox: to promote or to suppress? Free Radic. Biol. Med. 104 (2017 Mar) 144–164, https://doi.org/10.1016/j.freeradbiomed.2017.01.004.
[3] H. Yang, R.M. Villani, H. Wang, M.J. Simpson, M.S. Roberts, M. Tang, X. Liang, The role of cellular reactive oxygen species in cancer chemotherapy, J. Exp. Clin. Cancer Res. 37 (1) (2018 Nov 1) 266, https://doi.org/10.1186/s13046-018-0909-x.
[4] V.I. Sayin, M.X. Ibrahim, E. Larsson, J.A. Nilsson, P. Lindahl, M.O. Bergo, Antioxidants accelerate lung cancer progression in mice, Sci. Transl. Med. 6 (221) (2014 Jan 29) 221ra15, https://doi.org/10.1126/scitranslmed.3007653.
[5] Y. Shi, F. Nikulenkov, J. Zawacka-Pankau, H. Li, R. Gabdoulline, J. Xu, S. Eriksson, E. Hedström, N. Issaeva, A. Kel, E.S. Arnér, G. Selivanova, ROS-dependent activation of JNK converts p53 into an efficient inhibitor of oncogenes leading to robust apoptosis, Cell Death Differ. 21 (4) (2014 Apr) 612–623, https://doi.org/10.1038/cdd.2013.186.
[6] A. Kauppinen, T. Suuronen, J. Ojala, K. Kaarniranta, A. Salminen, Antagonistic crosstalk between NF-κB and SIRT1 in the regulation of inflammation and metabolic disorders, Cell. Signal. 25 (10) (2013 Oct) 1939–1948, https://doi.org/10.1016/j.cellsig.2013.06.007.
[7] J. Xie, X. Zhang, L. Zhang, Negative regulation of inflammation by SIRT1, Pharmacol. Res. 67 (1) (2013 Jan) 60–67, https://doi.org/10.1016/j.phrs.2012.10.010.
[8] W.R. Wang, T.T. Li, T. Jing, Y.X. Li, X.F. Yang, Y.H. He, W. Zhang, R. Lin, J.Y. Zhang, SIRT1 regulates the inflammatory response of vascular adventitial fibroblasts through autophagy and related signaling pathway, Cell. Physiol. Biochem. 41 (2) (2017) 569–582, https://doi.org/10.1159/000457878.
[9] K.C. Chang, P.F. Liu, C.H. Chang, Y.C. Lin, Y.J. Chen, C.W. Shu, The interplay of autophagy and oxidative stress in the pathogenesis and therapy of retinal degenerative diseases, Cell Biosci. 12 (1) (2022 Jan 3) 1, https://doi.org/10.1186/s13578-021-00736-9.
[10] M. Esquivel-Velázquez, P. Ostoa-Saloma, M.I. Palacios-Arreola, K.E. Nava-Castro, J.I. Castro, J. Morales-Montor, The role of cytokines in breast cancer development and progression, J. Interferon Cytokine Res. 35 (1) (2015 Jan) 1–16, https://doi.org/10.1089/jir.2014.0026.
[11] E. De Smaele, F. Zazzeroni, S. Papa, D.U. Nguyen, R. Jin, J. Jones, R. Cong, G. Franzoso, Induction of gadd45beta by NF-kappaB downregulates pro-apoptotic JNK signalling, Nature 414 (6861) (2001 Nov 15) 308–313, https://doi.org/10.1038/35104560.
[12] H. Nakano, Signaling crosstalk between NF-kappaB and JNK, Trends Immunol. 25 (8) (2004 Aug) 402–405, https://doi.org/10.1016/j.it.2004.05.007.
[13] S. Papa, F. Zazzeroni, C.G. Pham, C. Bubici, G. Franzoso, Linking JNK signaling to NF-kappaB: a key to survival, J. Cell Sci. 117 (Pt 22) (2004 Oct 15) 5197–5208, https://doi.org/10.1242/jcs.01483.
[14] X. Dai, C. Yin, Y. Zhang, G. Guo, C. Zhao, O. Wang, Y. Xiang, X. Zhang, G. Liang, Osthole inhibits triple negative breast cancer cells by suppressing STAT3, J. Exp. Clin. Cancer Res. 37 (1) (2018 Dec 22) 322, https://doi.org/10.1186/s13046-018-0992-z.
[15] A.K. Esnakula, L. Ricks-Santi, J. Kwagyan, Y.M. Kanaan, R.L. DeWitty, L.L. Wilson, B. Gold, W.A. Frederick, T.J. Naab, Strong association of fascin expression with triple negative breast cancer and basal-like phenotype in African-American women, J. Clin. Pathol. 67 (2) (2014 Feb) 153–160, https://doi.org/10.1136/jclinpath-2013-201698.
[16] Y. Song, L. Qian, S. Song, L. Chen, Y. Zhang, G. Yuan, H. Zhang, Q. Xia, M. Hu, M. Yu, M. Shi, Z. Jiang, N. Guo, Fra-1 and Stat3 synergistically regulate activation of human MMP-9 gene, Mol. Immunol. 45 (1) (2008 Jan) 137–143, https://doi.org/10.1016/j.molimm.2007.04.031.
[17] Y. Takahashi, D. Coppola, N. Matsushita, H.D. Cualing, M. Sun, Y. Sato, C. Liang, J.U. Jung, J.Q. Cheng, J.J. Mulé, W.J. Pledger, H.G. Wang, Bif-1 interacts with Beclin 1 through UVRAG and regulates autophagy and tumorigenesis, Nat. Cell Biol. 9 (10) (2007 Oct) 1142–1151, https://doi.org/10.1038/ncb1634.
[18] H. Wang, S. Mannava, V. Grachtchouk, D. Zhuang, M.S. Soengas, A.V. Gudkov, E.V. Prochownik, M.A. Nikiforov, c-Myc depletion inhibits proliferation of human tumor cells at various stages of the cell cycle, Oncogene 27 (13) (2008 Mar 20) 1905–1915, https://doi.org/10.1038/sj.onc.1210823.
[19] K. Degenhardt, R. Mathew, B. Beaudoin, K. Bray, D. Anderson, G. Chen, C. Mukherjee, Y. Shi, C. Gélinas, Y. Fan, D.A. Nelson, S. Jin, E. White, Autophagy promotes tumor cell survival and restricts necrosis, inflammation, and tumorigenesis, Cancer Cell 10 (1) (2006 Jul) 51–64, https://doi.org/10.1016/j.ccr.2006.06.001.
[20] B.T. Hennessy, D.L. Smith, P.T. Ram, Y. Lu, G.B. Mills, Exploiting the PI3K/AKT pathway for cancer drug discovery, Nat. Rev. Drug Discov. 4 (12) (2005 Dec) 988–1004, https://doi.org/10.1038/nrd1902.
[21] D. Morgensztern, H.L. McLeod, PI3K/Akt/mTOR pathway as a target for cancer therapy, Anti Cancer Drugs 16 (8) (2005 Sep) 797–803, https://doi.org/10.1097/01.cad.0000173476.67239.3b.
[22] S. Arico, A. Petiot, C. Bauvy, P.F. Dubbelhuis, A.J. Meijer, P. Codogno, E. Ogier-Denis, The tumor suppressor PTEN positively regulates macroautophagy by inhibiting the phosphatidylinositol 3-kinase/protein kinase B pathway, J. Biol. Chem. 276 (38) (2001 Sep 21) 35243–35246, https://doi.org/10.1074/jbc.C100319200.
[23] B.R. Pires, A.L. Mencalha, G.M. Ferreira, W.F. de Souza, J.A. Morgado-Díaz, A.M. Maia, S. Corrêa, E.S. Abdelhay, NF-kappaB is involved in the regulation of EMT genes in breast cancer cells, PLoS One 12 (1) (2017 Jan 20), e0169622, https://doi.org/10.1371/journal.pone.0169622.
[24] V. Srinivasan, W.D. Spence, S.R. Pandi-Perumal, R. Zakharia, K.P. Bhatnagar, A. Brzezinski, Melatonin and human reproduction: shedding light on the darkness hormone, Gynecol. Endocrinol. 25 (12) (2009 Dec) 779–785, https://doi.org/10.3109/09513590903159649.
[25] M. Szkiela, E. Kusideł, T. Makowiec-Dąbrowska, D. Kaleta, Night shift work-A risk factor for breast cancer, Int. J. Environ. Res. Publ. Health 17 (2) (2020 Jan 20) 659, https://doi.org/10.3390/ijerph17020659.
[26] J. Tong, S. Sheng, Y. Sun, H. Li, W.P. Li, C. Zhang, Z.J. Chen, Melatonin levels in follicular fluid as markers for IVF outcomes and predicting ovarian reserve, Reproduction 153 (4) (2017 Apr) 443–451, https://doi.org/10.1530/REP-16-0641.
[27] C. Karaaslan, S. Suzen, Antioxidant properties of melatonin and its potential action in diseases, Curr. Top. Med. Chem. 15 (9) (2015) 894–903, https://doi.org/10.2174/1568026615666150220120946.
[28] H. Ahabrach, N. El Mlili, M. Errami, O. Cauli, Circadian rhythm and concentration of melatonin in breast cancer patients, Endocr., Metab. Immune Disord.: Drug Targets 21 (10) (2021) 1869–1881, https://doi.org/10.2174/1871530320666201201110807.

[29] Y.H. Shih, K.C. Chiu, T.H. Wang, W.C. Lan, B.H. Tsai, L.J. Wu, S.M. Hsia, T.M. Shieh, Effects of melatonin to arecoline-induced reactive oxygen species production and DNA damage in oral squamous cell carcinoma, J. Formos. Med. Assoc. 120 (1 Pt 3) (2021 Jan) 668–678, https://doi.org/10.1016/j.jfma.2020.07.037.

[30] J. Florido, L. Martinez-Ruiz, C. Rodriguez-Santana, A. López-Rodríguez, A. Hidalgo-Gutiérrez, C. Cottet-Rousselle, F. Lamarche, U. Schlattner, A. Guerra-Librero, P. Aranda-Martínez, D. Acuña-Castroviejo, L.C. López, G. Escames, Melatonin drives apoptosis in head and neck cancer by increasing mitochondrial ROS generated via reverse electron transport, J. Pineal Res. 73 (3) (2022 Oct), e12824, https://doi.org/10.1111/jpi.12824.

[31] S. Mukherjee, S. Ghosh, S. Choudhury, P. Gupta, A. Adhikary, S. Chattopadhyay, Pomegranate polyphenols attenuate inflammation and hepatic damage in tumor-bearing mice: crucial role of NF-κB and the Nrf2/GSH Axis, J. Nutr. Biochem. 97 (2021 Nov), 108812, https://doi.org/10.1016/j.jnutbio.2021.108812.

[32] M. Ahir, S. Bhattacharya, S. Karmakar, A. Mukhopadhyay, S. Mukherjee, S. Ghosh, S. Chattopadhyay, P. Patra, A. Adhikary, Tailored-CuO-nanowire decorated with folic acid mediated coupling of the mitochondrial-ROS generation and miR425-PTEN axis in furnishing potent anti-cancer activity in human triple negative breast carcinoma cells, Biomaterials 76 (2016 Jan) 115–132, https://doi.org/10.1016/j.biomaterials.2015.10.044.

[33] B. Kocatürk, H.H. Versteeg, Orthotopic injection of breast cancer cells into the mammary fat pad of mice to study tumor growth, J. Vis. Exp. (96) (2015 Feb 8), 51967, https://doi.org/10.3791/51967.

[34] B.V. Jardim-Perassi, A.S. Arbab, L.C. Ferreira, T.F. Borin, N.R. Varma, A.S. Iskander, A. Shankar, M.M. Ali, D.A. de Campos Zuccari, Effect of melatonin on tumor growth and angiogenesis in xenograft model of breast cancer, PLoS One 9 (1) (2014 Jan 9), e85311, https://doi.org/10.1371/journal.pone.0085311.

[35] S. Choudhury, S. Ghosh, P. Gupta, S. Mukherjee, S. Chattopadhyay, Inflammation-induced ROS generation causes pancreatic cell death through modulation of Nrf2/NF-κB and SAPK/JNK pathway, Free Radic. Res. 49 (11) (2015) 1371–1383, https://doi.org/10.3109/10715762.2015.1075016.

[36] S. Ghosh, S. Mukherjee, S. Choudhury, P. Gupta, A. Adhikary, R. Baral, S. Chattopadhyay, Reactive oxygen species in the tumor niche triggers altered activation of macrophages and immunosuppression: role of fluoxetine, Cell. Signal. 27 (7) (2015 Jul) 1398–1412, https://doi.org/10.1016/j.cellsig.2015.03.013.

[37] L. DeVorkin, S.M. Gorski, LysoTracker staining to aid in monitoring autophagy in Drosophila, Cold Spring Harb. Protoc. 2014 (9) (2014 Sep 2) 951–958, https://doi.org/10.1101/pdb.prot080325.

[38] S. Chikte, N. Panchal, G. Warnes, Use of LysoTracker dyes: a flow cytometric study of autophagy, Cytometry 85 (2) (2014 Feb) 169–178, https://doi.org/10.1002/cyto.a.22312.

[39] Z. Jamal, J. Das, P. Gupta, P. Dhar, S. Chattopadhyay, U. Chatterji, Self Nano-Emulsifying Curcumin (SNEC30) attenuates arsenic-induced cell death in mice, Toxicol Rep 8 (2021 Jul 17) 1428–1436, https://doi.org/10.1016/j.toxrep.2021.07.010.

[40] M. Izdebska, M. Hałas-Wiśniewska, W. Zielińska, A. Klimaszewska-Wiśniewska, D. Grzanka, M. Gagat, Lidocaine induces protective autophagy in rat C6 glioma cell line, Int. J. Oncol. 54 (3) (2019 Mar) 1099–1111, https://doi.org/10.3892/ijo.2018.4668.

[41] P. Gupta, S. Choudhury, S. Ghosh, S. Mukherjee, O. Chowdhury, A. Sain, S. Chattopadhyay, Dietary pomegranate supplement alleviates murine pancreatitis by modulating Nrf2-p21 interaction and controlling apoptosis to survival switch, J. Nutr. Biochem. 66 (2019 Apr) 17–28, https://doi.org/10.1016/j.jnutbio.2018.12.009.

[42] E.A. Rakha, J.S. Reis-Filho, F. Baehner, D.J. Dabbs, T. Decker, V. Eusebi, S.B. Fox, S. Ichihara, J. Jacquemier, S.R. Lakhani, J. Palacios, A.L. Richardson, S. J. Schnitt, F.C. Schmitt, P.H. Tan, G.M. Tse, S. Badve, I.O. Ellis, Breast cancer prognostic classification in the molecular era: the role of histological grade, Breast Cancer Res. 12 (4) (2010) 207, https://doi.org/10.1186/bcr2607.

[43] K.J. Winzer, A. Buchholz, M. Schumacher, W. Sauerbrei, Improving the Prognostic Ability through Better Use of Standard Clinical Data - The Nottingham Prognostic Index as an Example, PLoS One 11 (3) (2016), e0149977, https://doi.org/10.1371/journal.pone.0149977.

[44] D.N. Dhanasekaran, E.P. Reddy, JNK-signaling: a multiplexing hub in programmed cell death, Genes Cancer 8 (9–10) (2017 Sep) 682–694, https://doi.org/10.18632/genesandcancer.155.

[45] R. Salgado, S. Junius, I. Benoy, P. Van Dam, P. Vermeulen, E. Van Marck, P. Huget, L.Y. Dirix, Circulating interleukin-6 predicts survival in patients with metastatic breast cancer, Int. J. Cancer 103 (5) (2003 Feb 20) 642–646, https://doi.org/10.1002/ijc.10833.

[46] I. Segatto, G. Baldassarre, B. Belletti, STAT3 in breast cancer onset and progression: a matter of time and context, Int. J. Mol. Sci. 19 (9) (2018 Sep 18) 2818, https://doi.org/10.3390/ijms19092818.

[47] Q. Chang, L. Daly, J. Bromberg, The IL-6 feed-forward loop: a driver of tumorigenesis, Semin. Immunol. 26 (1) (2014 Feb) 48–53, https://doi.org/10.1016/j.smim.2014.01.007.

[48] S. Chung, H. Yao, S. Caito, J.W. Hwang, G. Arunachalam, I. Rahman, Regulation of SIRT1 in cellular functions: role of polyphenols, Arch. Biochem. Biophys. 501 (1) (2010 Sep 1) 79–90, https://doi.org/10.1016/j.abb.2010.05.003.

[49] W.R. Wang, T.T. Li, T. Jing, Y.X. Li, X.F. Yang, Y.H. He, W. Zhang, R. Lin, J.Y. Zhang, SIRT1 regulates the inflammatory response of vascular adventitial fibroblasts through autophagy and related signaling pathway, Cell. Physiol. Biochem. 41 (2) (2017) 569–582, https://doi.org/10.1159/000457878.

[50] I.H. Lee, L. Cao, R. Mostoslavsky, D.B. Lombard, J. Liu, N.E. Bruns, M. Tsokos, F.W. Alt, T. Finkel, A role for the NAD-dependent deacetylase Sirt1 in the regulation of autophagy, Proc Natl Acad Sci U S A 105 (9) (2008 Mar 4) 3374–3379, https://doi.org/10.1073/pnas.0712145105.

[51] N. Hariharan, Y. Maejima, J. Nakae, J. Paik, R.A. Depinho, J. Sadoshima, Deacetylation of FoxO by Sirt1 plays an essential role in mediating starvation-induced autophagy in cardiac myocytes, Circ. Res. 107 (12) (2010 Dec 10) 1470–1482, https://doi.org/10.1161/CIRCRESAHA.110.227371.

[52] Z. Tan, H. Xue, Y. Sun, C. Zhang, Y. Song, Y. Qi, The role of tumor inflammatory microenvironment in lung cancer, Front. Pharmacol. 12 (2021 May 17), 688625, https://doi.org/10.3389/fphar.2021.688625.

[53] H. Wei, S. Wei, B. Gan, X. Peng, W. Zou, J.L. Guan, Suppression of autophagy by FIP200 deletion inhibits mammary tumorigenesis, Genes Dev. 25 (14) (2011 Jul 15) 1510–1527, https://doi.org/10.1101/gad.2051011.

[54] A. Salminen, K. Kaarniranta, A. Kauppinen, Beclin 1 interactome controls the crosstalk between apoptosis, autophagy and inflammasome activation: impact on the aging process, Ageing Res. Rev. 12 (2) (2013 Mar) 520–534, https://doi.org/10.1016/j.arr.2012.11.004.

[55] A. Sakatani, F. Sonohara, A. Goel, Melatonin-mediated downregulation of thymidylate synthase as a novel mechanism for overcoming 5-fluorouracil associated chemoresistance in colorectal cancer cells, Carcinogenesis 40 (2019) 422–431, https://doi.org/10.1093/carcin/bgy186.

[56] Z. Liu, X. Sang, M. Wang, Y. Liu, J. Liu, X. Wang, P. Liu, H. Cheng, Melatonin potentiates the cytotoxic effect of Neratinib in HER2+ breast cancer through promoting endocytosis and lysosomal degradation of HER2, Oncogene 40 (2021) 6273–6283, https://doi.org/10.1038/s41388-021-02015-w.

[57] P.F. Innominato, A.S. Lim, O. Palesh, M. Clemons, M. Trudeau, A. Eisen, C. Wang, A. Kiss, K.I. Pritchard, G.A. Bjarnason, The effect of melatonin on sleep and quality of life in patients with advanced breast cancer, Supportive Care Cancer Off. J. Multinatl. Assoc. Supportive Care Cancer. 24 (2016) 1097–1105, https://doi.org/10.1007/s00520-015-2883-6.

[58] C. Alonso-González, A. González, J. Menéndez-Menéndez, C. Martínez-Campa, S. Cos, Melatonin as a radio-sensitizer in cancer, Biomedicines 8 (2020) 247, https://doi.org/10.3390/biomedicines8080247.

[59] M. Zhang, R. Li, R. Zhang, Y. Zhang, Melatonin sensitizes esophageal cancer cells to 5-fluorouracil via promotion of apoptosis by regulating EZH2 expression, Oncol. Rep. 45 (2021) 22, https://doi.org/10.3892/or.2021.7973.

[60] Y. Zhao, C. Wang, A. Goel, A combined treatment with melatonin and andrographis promotes autophagy and anti-cancer activity in colorectal cancer, Carcinogenesis (2022) bgac008, https://doi.org/10.1093/carcin/bgac008.

[61] A. Lozano, J. Marruecos, J. Rubió, N. Farré, J. Gómez-Millán, R. Morera, I. Planas, M. Lanzuela, M.G. Vázquez-Masedo, L. Cascallar, et al., Randomized placebo-controlled phase II trial of high-dose melatonin mucoadhesive oral gel for the prevention and treatment of oral mucositis in patients with head and neck cancer undergoing radiation therapy concurrent with systemic treatment, Clin. Transl. Oncol. 23 (2021) 1801–1810, https://doi.org/10.1007/s12094-021-02586-w.

[62] Q.H. Tran, D.H. Hoang, M. Song, W. Choe, I. Kang, S.S. Kim, J. Ha, Melatonin and doxorubicin synergistically enhance apoptosis via autophagy-dependent reduction of AMPKα1 transcription in human breast cancer cells, Exp. Mol. Med. 53 (2021) 1413–1422, https://doi.org/10.1038/s12276-021-00675-y.

[63] N.G. Harpsøe, L.P.H. Andersen, I. Gögenur, J. Rosenberg, Clinical pharmacokinetics of melatonin: a systematic review, Eur. J. Clin. Pharmacol. 71 (2015) 901–909, https://doi.org/10.1007/s00228-015-187.

[64] L. Wang, C. Wang, W.S. Choi, Use of melatonin in cancer treatment: where are we? Int. J. Mol. Sci. 23 (7) (2022 Mar 29) 3779, https://doi.org/10.3390/ijms23073779. PMID: 35409137; PMCID: PMC8998229.

[65] A.A. Hashmi, K.A. Hashmi, M. Irfan, S.M. Khan, M.M. Edhi, J.P. Ali, S.K. Hashmi, H. Asif, N. Faridi, A. Khan, Ki67 index in intrinsic breast cancer subtypes and its association with prognostic parameters, BMC Res. Notes 12 (1) (2019 Sep 23) 605, https://doi.org/10.1186/s13104-019-4653-x.
[66] G.Ö. Önder, G. Sezer, S. Özdamar, A. Yay, Melatonin has an inhibitory effect on MCF-7 and MDA-MB-231 human breast cancer cell lines by inducing autophagy and apoptosis, Fundam. Clin. Pharmacol. (2022 Jul 2), https://doi.org/10.1111/fcp.12813.
[67] L. Bosch-Presegué, A. Vaquero, The dual role of sirtuins in cancer, Genes Cancer 2 (6) (2011 Jun) 648–662, https://doi.org/10.1177/1947601911417862.
[68] M.K. Han, E.K. Song, Y. Guo, X. Ou, C. Mantel, H.E. Broxmeyer, SIRT1 regulates apoptosis and Nanog expression in mouse embryonic stem cells by controlling p53 subcellular localization, Cell Stem Cell 2 (3) (2008 Mar 6) 241–251, https://doi.org/10.1016/j.stem.2008.01.002.
[69] Verzella D, Pescatore A, Capece D, Vecchiotti D, Ursini MV, Franzoso G, Alesse E, Zazzeroni F. Life, death, and autophagy in cancer: NF-κB turns up everywhere. Cell Death Dis. 2020 Mar 30;11(3):210. doi: 10.1038/s41419-020-2399-y. PMID: 32231206; PMCID: PMC7105474.
[70] M. Karin, NF-kappaB as a critical link between inflammation and cancer, Cold Spring Harb Perspect Biol 1 (5) (2009 Nov) a000141, https://doi.org/10.1101/cshperspect.a000141.
[71] M.K. Wendt, N. Balanis, C.R. Carlin, W.P. Schiemann, STAT3 and epithelial-mesenchymal transitions in carcinomas, JAK-STAT 3 (1) (2014 Jan 1), e28975, https://doi.org/10.4161/jkst.28975.
[72] H. Chen, Z. Yang, C. Ding, L. Chu, Y. Zhang, K. Terry, H. Liu, Q. Shen, J. Zhou, Fragment-based drug design and identification of HJC0123, a novel orally bioavailable STAT3 inhibitor for cancer therapy, Eur. J. Med. Chem. 62 (2013 Apr) 498–507, https://doi.org/10.1016/j.ejmech.2013.01.023.
[73] B. Kocatürk, H.H. Versteeg, Orthotopic injection of breast cancer cells into the mammary fat pad of mice to study tumor growth, J. Vis. Exp. (96) (2015 Feb 8), 51967, https://doi.org/10.3791/51967.
[74] E. Oh, Y.J. Kim, H. An, D. Sung, T.M. Cho, L. Farrand, S. Jang, J.H. Seo, J.Y. Kim, Flubendazole elicits anti-metastatic effects in triple-negative breast cancer via STAT3 inhibition, Int. J. Cancer 143 (8) (2018 Oct 15) 1978–1993, https://doi.org/10.1002/ijc.31585.
[75] S.F. Hendrayani, B. Al-Harbi, M.M. Al-Ansari, G. Silva, A. Aboussekhra, The inflammatory/cancer-related IL-6/STAT3/NF-κB positive feedback loop includes AUF1 and maintains the active state of breast myofibroblasts, Oncotarget 7 (27) (2016 Jul 5) 41974–41985, https://doi.org/10.18632/oncotarget.9633.
[76] S. Pattingre, A. Tassa, X. Qu, R. Garuti, X.H. Liang, N. Mizushima, M. Packer, M.D. Schneider, B. Levine, Bcl-2 antiapoptotic proteins inhibit Beclin 1-dependent autophagy, Cell 122 (6) (2005 Sep 23) 927–939, https://doi.org/10.1016/j.cell.2005.07.002.
[77] M.C. Maiuri, G. Le Toumelin, A. Criollo, J.C. Rain, F. Gautier, P. Juin, E. Tasdemir, G. Pierron, K. Troulinaki, N. Tavernarakis, J.A. Hickman, O. Geneste, G. Kroemer, Functional and physical interaction between Bcl-X(L) and a BH3-like domain in Beclin-1, EMBO J. 26 (10) (2007 May 16) 2527–2539, https://doi.org/10.1038/sj.emboj.7601689.
[78] L. Kma, T.J. Baruah, The interplay of ROS and the PI3K/Akt pathway in autophagy regulation, Biotechnol. Appl. Biochem. 69 (1) (2022 Feb) 248–264, https://doi.org/10.1002/bab.2104.
[79] A. Takeda-Watanabe, M. Kitada, K. Kanasaki, D. Koya, SIRT1 inactivation induces inflammation through the dysregulation of autophagy in human THP-1 cells, Biochem. Biophys. Res. Commun. 427 (1) (2012 Oct 12) 191–196, https://doi.org/10.1016/j.bbrc.2012.09.042.
[80] C. Nopparat, P. Sinjanakhom, P. Govitrapong, Melatonin reverses H_2O_2 -induced senescence in SH-SY5Y cells by enhancing autophagy via sirtuin 1 deacetylation of the RelA/p65 subunit of NF-κB, J. Pineal Res. 63 (1) (2017 Aug), https://doi.org/10.1111/jpi.12407.
[81] H.J. Hugo, M.I. Kokkinos, T. Blick, M.L. Ackland, E.W. Thompson, D.F. Newgreen, Defining the E-cadherin repressor interactome in epithelial-mesenchymal transition: the PMC42 model as a case study, Cells Tissues Organs 193 (1–2) (2011) 23–40, https://doi.org/10.1159/000320174.
[82] A. Børretzen, K. Gravdal, S.A. Haukaas, M. Mannelqvist, C. Beisland, L.A. Akslen, O.J. Halvorsen, The epithelial-mesenchymal transition regulators Twist, Slug, and Snail are associated with aggressive tumour features and poor outcome in prostate cancer patients, J Pathol Clin Res 7 (3) (2021) 253–270, https://doi.org/10.1002/cjp2.202. Epub 2021 Feb 19. PMID: 33605548; PMCID: PMC8073012.
[83] A. Puissant, N. Fenouille, P. Auberger, When autophagy meets cancer through p62/SQSTM1, Am. J. Cancer Res. 2 (4) (2012) 397–413.
[84] Y. Katsuragi, Y. Ichimura, M. Komatsu, p62/SQSTM1 functions as a signaling hub and an autophagy adaptor, FEBS J. 282 (24) (2015 Dec) 4672–4678, https://doi.org/10.1111/febs.13540.
[85] G. Schimmack, K. Schorpp, K. Kutzner, T. Gehring, J.K. Brenke, K. Hadian, D. Krappmann, YOD1/TRAF6 association balances p62-dependent IL-1 signaling to NF-kappaB, Elife 6 (2017), e22416, https://doi.org/10.7554/eLife.22416.
[86] S. Yang, L. Qiang, A. Sample, P. Shah, Y.Y. He, NF-κB signaling activation induced by chloroquine requires autophagosome, p62 protein, and c-jun N-terminal kinase (JNK) signaling and promotes tumor cell resistance, J. Biol. Chem. 292 (8) (2017 Feb 24) 3379–3388, https://doi.org/10.1074/jbc.M116.756536.
[87] L. Qiang, B. Zhao, M. Ming, N. Wang, T.C. He, S. Hwang, A. Thorburn, Y.Y. He, Regulation of cell proliferation and migration by p62 through stabilization of Twist1, Proc Natl Acad Sci U S A 111 (25) (2014 Jun 24) 9241–9246, https://doi.org/10.1073/pnas.1322913111.
[88] B.R. Pires, A.L. Mencalha, G.M. Ferreira, W.F. de Souza, J.A. Morgado-Díaz, A.M. Maia, S. Corrêa, E.S. Abdelhay, NF-kappaB is involved in the regulation of EMT genes in breast cancer cells, PLoS One 12 (1) (2017 Jan 20), e0169622, https://doi.org/10.1371/journal.pone.0169622.